POLITECNICO DI TORINO

Master Course in Aerospace Engineering

Master Degree Thesis

Design and Development of an Electromechanical Test Bench for the Study of Optic Sensors

Supervisor:
Ing. Matteo Dalla Vedova

Co-Supervisor
Prof. Paolo Maggiore

Candidate:
Bruno Lavagnino

March 2019

Cominciate col fare ciò che è necessario, poi ciò che è possibile.
E all'improvviso vi sorprenderete a fare l'impossibile.

Abstract

The goal of this thesis is to test a new typology of fiber optic sensor: the Fiber Bragg Grating (FBG) on an flexed element.
The work has been achieved at the Aerospace Engineering Department of the Politecnico of Torino, in collaboration with the interdepartmental team Photonext and the Istituto Superiore Mario Boella.
During the discussion it is possible to see what the FBG and their properties are, what their big advantages would be and also their disadvantages.
The tools and the hardware that have been designed to test the FBG and the software used to process the output data will be listed.
This work is justified by the enormous advantages of the FBG used like sensors. They are lightweight and, since they work with light, they are indifferent to electromagnetic interferences. Furthermore, an optical fiber could have more Bragg Gratings inside itself, so it could make different measurements in different points, also of different physical phenomena. Hence, with only one optical fiber, temperatures, pressures, strains and vibrations could be detected, which brings great benefits to redundant the sensors of any engineering system. Lastly the FBG in itself does not need external power source, unlike to common electric sensors.

Abstract

L'obiettivo di questa trattazione è testare una nuova tipologia di sensori ottici: i sensori a reticolo di Bragg su un elemento sottoposto a flessione.
L'attività è stata svolta presso il Dipartimento di Ingegneria Aerospaziale del Politecnico di Torino, in collaborazione con il team interdipartimentale Photonext e l'Istituto Superiore Mario Boella.
Nella trattazione è possibile vedere cosa sono le Fibre con il reticolo di Bragg, quali sono le loro proprietà e quali potrebbero essere i loro potenziali vantaggi, ma anche le loro criticità.
Verranno poi elencati gli strumenti e le attrezzature usate ed i software richiesti per processare ed elaborare i dati.
Il lavoro è giustificato dagli enormi vantaggi dei FBG usati come sensori. Sono leggeri e, siccome operano con la luce, sono insensibili ai disturbi elettromagnetici. Inoltre una fibra ottica può avere più reticoli di Bragg al suo interno, così può effettuare diverse misurazioni in diversi punti, anche di grandezze fisiche diverse. Perciò, con una sola fibra ottica, si possono misurare temperature, pressioni, deformazioni e vibrazioni, il che porta notevoli vantaggi nella ridondanza di sensori di un qualsiasi sistema ingegneristico. In ultimo si tenga presente che il FBG in sé non ha bisogno di una sorgente di potenza, a differenza dei comuni sensori elettrici.

Acknowledgements

I would like to thank many people. At first my supervisor, Ing. Matteo Dalla Vedova and the co-supervisors, Prof. Paolo Maggiore. Then the Ing. Piercarlo Berri and Ing. Matteo Facciano.
I could not forget my colleagues of the team Photonext and I want to thank all the people that I met during my academic career.
The biggest thank is for my family and I need of thanks all the other people who have helped me during my route.

Ringraziamenti

Arrivato alla conclusione della tesi ho molte persone da ringraziare. Innanzitutto il mio relatore, Ing Matteo Dalla Vedova, ed il mio co-relatore, il Prof. Paolo Maggiore. Desidero ringraziare anche l'Ing. Piercarlo Berri e l'Ing. Matteo Facciano, sempre disponibili a fornirci assistenza.
Inoltre ci tengo a ringraziare tutti i colleghi con cui abbiano condiviso questa esperienza: compagni di corso, compagni di ateneo e colleghi tesisti,
Ma il ringraziamento più grande va alla mia famiglia, che mi ha sempre sostenuto, incoraggiato e spinto ad andare avanti nonostante gli imprevisti del percorso.

Contents

List of figures

List of tables

1 Introduction

Optical Fiber sensors are new interesting measuring devices, which can be used to make different type of measures. This happens thanks to the way in which the light passes through the fiber. The light is insensitive to the electromagnetic disturbances. Furthermore, FBG needs only a device that generates a signal of light and it can read its reflection coming back, but FBG in itself does not need a power source.

1.1 Objective of the Thesis

Our objective is to test the FBG like a strain sensing instrumentation. In some earlier works the FBG has been tested using traction: it has been glued on two plates, one fixed and one mounted on a micro translation, and it has been pulled.
Now the fiber is glued onto a sample comparable to a beam; hence the beam is flexed with a deformation imposed at the tip. The final deformation imposed to the samples will be 20mm, with 10 steps 2mm each one. When the tip reaches the position actuated, it stops itself for 30 seconds, then it restarts.
The measurements of the strain are detected and compared with the outputs of FEM analysis and, later, they are compared with the results given by the strain gauge.
After the FBG has been validated, some possible regards will be made about the weaknesses of this kind of sensors and the possible solutions.

1.2 Structure of the Thesis

After this chapter Fiber Optic and their Bragg Grating will be described. It will be possible to see what these Fiber are, their properties, how they are made and how the signals pass inside them. After this it will be shown what the grid of Bragg, called Bragg Grating, consists of. This grid gives to the fiber the ability to make measurements of various type.
The third chapter deals with fixtures and tools, from the test bench to the supports for the samples. Similarly in the fourth chapter the software used during the work will be listed.

In the fifth chapter it is possible to see the outputs of the tests, with tables and graphs to show clearly our results and get to the conclusion: is the Fiber Bragg Grating reliable? Is it handy to install and to use? Which criticalities has it?
This thesis tries to answer these questions in order to let this work to someone else that will carry it on in the future.

2 Fiber Optic and Bragg Grating, what are they?

2.1 Fiber Optic

Currently the optical fibers are widely used in the telecommunications. This is due to the very low attenuation of the signal that could achieve a value of 0.2 $dBkm^{-1}$.

2.1.1 Main Structure

Fiber optic is composed by a system of three concentric rings.
The most internal is the core, where the light passes through. Than the intermediate layer is the cladding, lastly there is the coating that has a protection function. The FBGs used for the thesis are acrylate fiber with the following diameters:

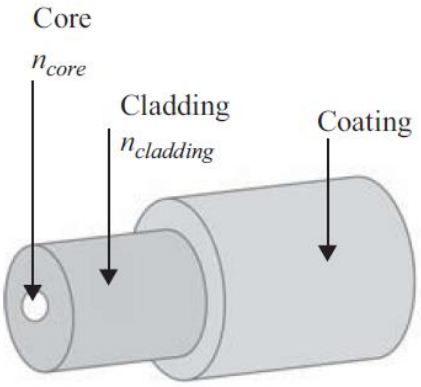

Figure 2.1 - Basic geometry of fiber optic [2]

Coating = 200 µm
Cladding = 125 µm
Core = 9 µm

The operating principle is based on the different reflex index between the core and the cladding:

$$n_{core} > n_{cladding} \tag{1}$$

When a ray of light strikes the boundary interface and the angle of incidence is larger than the critical angle, the light would be trapped in the fiber, and it passes through the core [2].
The equation (2) provides the refractive index:

$$n = \frac{c}{v} \tag{2}$$

- c = speed of light in vacuum
- v = speed of light in medium

There is a limit to the angle of strike of the light with the fiber. This limit derives by Shell's law:

$$n_1 sen\alpha_i = n_2 sen\alpha_r \tag{3}$$

The values are:

- $n_{1,2}$ = refractive index, respectively, of the first and the second medium
- α_i = incidence angle
- α_r = refractive angle

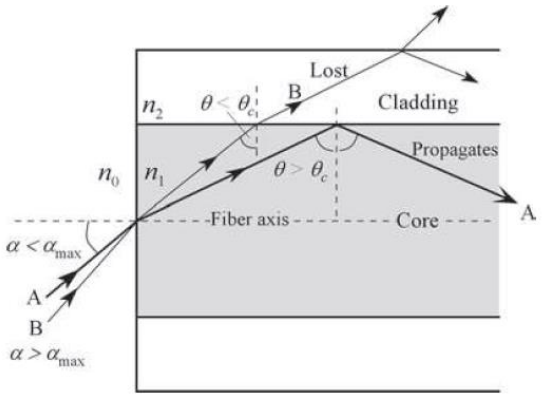

Figure 2.2 - Scheme of a fiber with the distinctive angles of the acceptance and propagation of the light [3]

Hence, there is a Critic Angle θ_c of transit of the light in the core, and the angle is function of the refractive indexes of the core and the cladding.
There is also a maximum Acceptance Angle α_{max}, that is the maximum angle that the light can have when it strikes the boundary of the fiber. It is derived from the following equations [3]:

$$n_0 sen(\alpha) = n_1 \left(\frac{\pi}{2} - \theta_c\right) \tag{4}$$

$$n_1 sen(\theta_c) = n_2 \left(\frac{\pi}{2}\right) \tag{5}$$

$$sen\ \alpha_{max} = \frac{\nu\sqrt{n_1^2 - n_2^2}}{n_0} \tag{6}$$

The factors n_0, n_1 and n_2 are, respectively, the refractive index of the external medium (air), of the core and of the cladding.
Then, in the hypothetical event n_1 and n_2 are equal, the light can pass through the fiber only in the parallel direction with the core. Otherwise, the more the refractive indexes are different the more the Acceptance Angle will be bigger. However, in this case, the light has to transit in the fiber with very irregular movement.

2.1.2 Material of the Fiber Optic

There are three factors to consider in order to choose the best performance material for fiber optics: weakness, cost and transmission optical loss. You can choose between two kind of fiber optics: the plastic optical fibers (POF) and the glass fibers.
[4] The POF are cheaper and more flexible, but they have high attenuation.
Instead, the glass fibers have a very low transmission optical loss, but they are more expensive and more weak. Furthermore, glass can be doped to increase or to reduce refraction index. Chemicals like Germanium dioxide (GeO_2), Phosphorus pentoxide (P_2O_5), Titanium dioxide (TiO_2) and Aluminum oxide (Al_2O_3) increase refraction index, so they are used to dope the core. On the other side, Boron trioxide (B_2O_3) and Fluorine (F) decrease the refraction index so you can use them for the cladding.
Obviously the selection of the kind of fiber depends on the purposes of the application: for example for short distance applications POF are used, instead, glass fibers are used for long distance applications.

2.2 Bragg Grating

Remote sensors systems give us the possibility to make measurements without actually being on site. [1] They can be grouped in two categories: active and passive sensors. In the active sensors the measuring system emits energy that “illuminates” the target, and receives part of its own energy reflected or scattered by the target. In the passive sensors, instead,

the equipment used to acquire the information from the target gathers the data from the natural energy emitted and/or reflected by the target.
In the previous section the fiber optics have been introduced. In the field of telecommunication, the core is made as more uniform as possible along its length. But if fiber optics are used as sensors, some periodical variations of the refractive index of the core are put along the length of the fiber to obtain a Bragg grating. It consists of a segment of the core which is "engraved" with a laser. The laser is modulated in the space and it changes locally the refraction index of the core. When the light, passing through the core, reaches the segment engraved, it will be reflected by the Bragg grating and it comes back. Hence, the Bragg gratin is exactly the sensor.

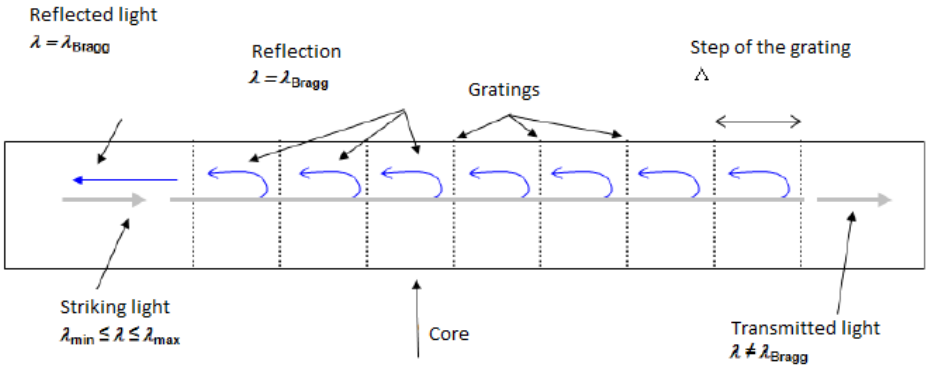

Figure 2.3 - Scheme of Bragg grating with the movements of the light [5]

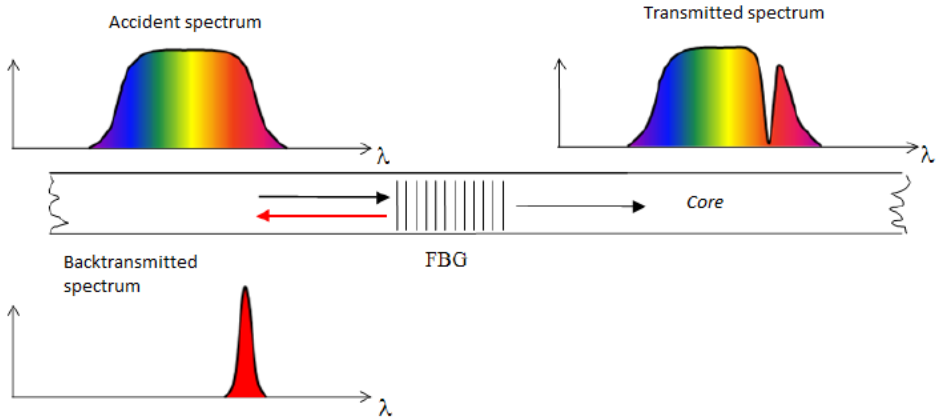

Figure 2.4 - Scheme of the behaviour of the light which strikes the FBG [5]

[4] The Behaviour of FBG is regulated by this fundamental equation:

$$\lambda_B = 2n_{eff}\Lambda \tag{7}$$

With:

- λ_B = Bragg wavelength
- n_{eff} = effective index of the grating
- Λ = Grating period

When the fiber optic undergoes variations of temperature, strain, pressure or vibrational motions, the λ_B changes.
Regarding the strain, if you know the properties of the fiber, the λ_B at rest and the variation of $\Delta\lambda_B$, the strain ϵ is immediately found from the following equation(8):

$$\Delta\lambda_B = \lambda_B \Big[\ 1 - P_e\ \epsilon + (\alpha_f + \zeta_f)\Delta T\Big] \tag{8}$$

Where P_e is the photoelasticy constant (0.22), ΔT is the variation of temperature, ζ_f is the thermo-optic coefficient and α_f is the thermal expansion coefficient of fiber optic.
The second open bracket contains the term regarding the thermal measures. This section is not subject of interest in this work.
This sub-chapter is fundamental and enough to the understanding of the work. At the end only the (8) has been used to analyse the strains of the FBGs and, consequently, of the samples. The equation allows to switch from the wavelength of FBGs to the strains.

2.2.1 Fabrication Techniques of the FBGs

There are some techniques to print the fiber optic and to make the Bragg Gratins [9]:

- **Single-beam internal technique**: in this process a single laser beam is launched into a germanium-doped silica fiber. The laser beam is generated by an argon-ion laser. The refractive index of the fiber is modified locally in the region of high intensity. Initially the reflectivity is low (4%) but it increases quickly thanks to the light reflected from the far end of the fiber and propagating in the backward direction. This process of continuous feedback makes the pro-

cess exponentially faster. The disadvantage of this technique is that grating can be used only near the wavelength of the laser used to make it.

- **Dual-beam holographic technique**: in this method a leaser generates two optical beams, it operates in ultraviolet region. It makes an angle of 2ϑ and it exposes the core of the fiber.

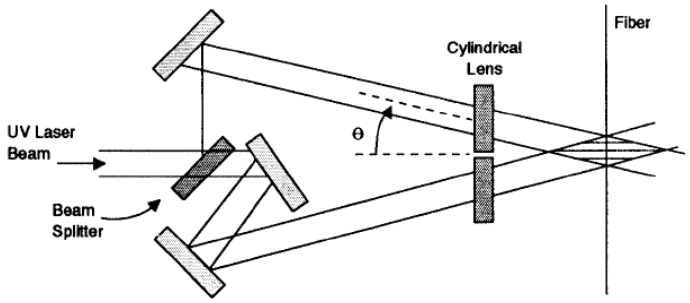

Figure 2.5 - Schematic illustration of the dual-beam holographic technique

Some cylinder lens are used to expand the beam along the fiber length. The advantage of this method is the possibility of make the grating period, which can be varied over a wide range by simply adjusting the angle ϑ.

- **Phase mask technique**: this technique is commonly used to make integrated electronic circuits.

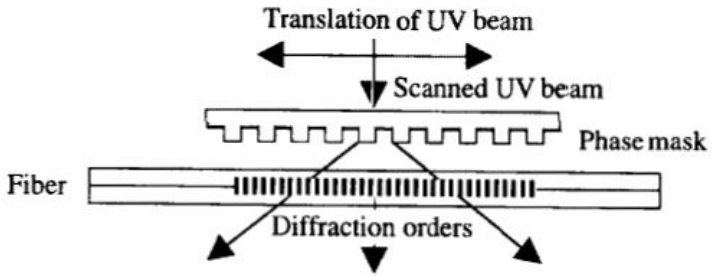

Figure 2.6 - - Schematic illustration of the phase mask technique

The phase mask acts as a master grating that is transferred to the fiber using a suitable method. The phase variations induced in the 242 nm radiation passing through the phase mask translate into a

periodic intensity patter similar to that produced by the holographic technique. Photosensitivity of the fiber converts intensity variations into an index grating of the same periodicity as that of the phase mask. This technique is much less stringent than the others, in terms of time and space, thanks to the noninterferometric nature of the method.

- **Point-by-point fabrication technique**: this technique goes beyond the phase mask method. It makes the gratings directly on the fiber, period by period, by exposing short section to a single high energy pulse. Than the fiber is translated by a distance Λw before the next pulse arrives.

  This technique has some limitations. At first the only short fiber gratings are produced for the high time-consuming nature of the method. Secondly it is hard to control the translation of the fiber accurately. Finally it is also hard to focus the laser beam to a small spot size that is only a fraction of the grating period.
- **Technique based on ultrashort optical pulse**: in this method you use the femtosecond pulse to change the refractive index of the fiber.

3 Hardware and Tools

The hardware is composed by some devices:

1) Our FBGs
2) Sample
3) Adhesive, Araldite 2011
4) Test bench and breadboard
5) Faulhaber MCDC2805
6) Micropositioner
7) Supports
8) Interrogator
9) Strain gauge

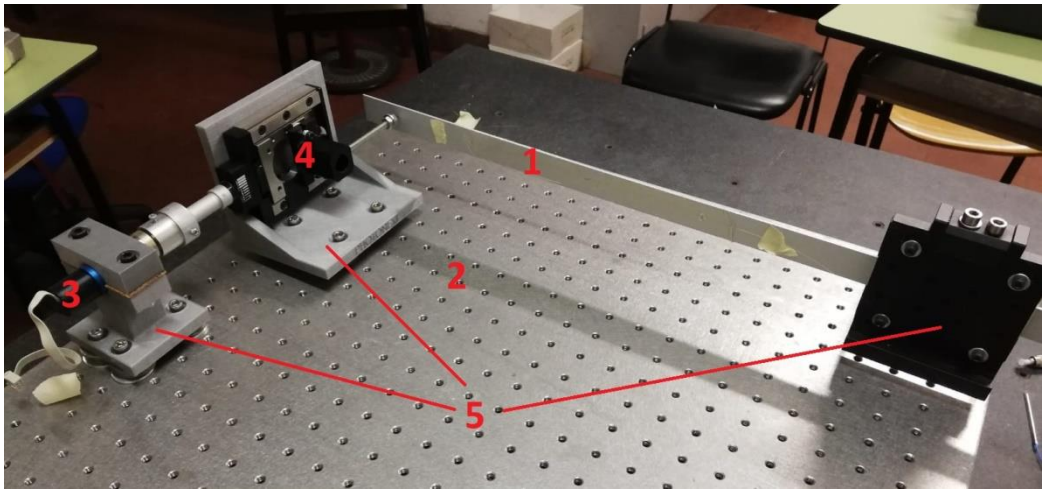

Figure 3.1 - Overview of the test bench assembled

3.1 Our FBGs

The FBGs in order to be connected to the Interrogator need a collector in an boundary of them. Moreover, in some tests you need fibers with more Bragg gratings on them. This joints have been made by engineer Matteo Facciano at Boella Institute.
In both cases the procedure is the following:

- Taking the two extremities which have to be jointed and removing the more external layer of the fiber, the coating. After this, you have to clean both the extremities with apposite wipes which do not let residuals and isopropyl alcohol.
- Both the extremities have to be cut in the cleaver: this device cuts a small portion of the fiber and it allows to have the surface in the extremities perfectly perpendicular to the core axis.

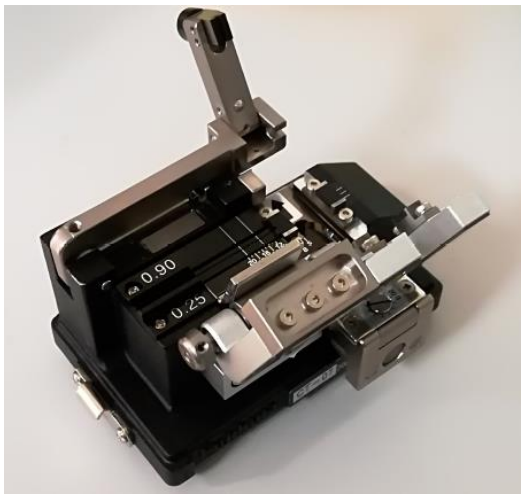

Figure 3.2 - The cleaver

- Now the two extremities pass into a splicer. Here they have been fixed like in the Figure 3.3, with the two extremities that have to be placed close. On the sides there are two electrodes, which will heat the extremities to glue them together.
  At this point you need only to close the device and it works automatically.

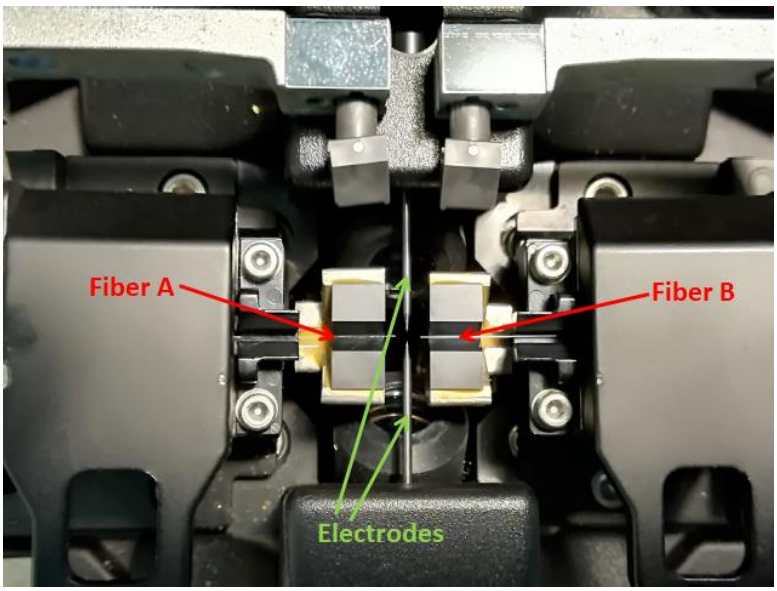

Figure 3.3 - The splicer

The splicer has a monitor that allows to see the operations of jointing.
Furthermore, it communicates if the junction has been brought to a successful conclusion and how much the loss signal of the joint is.

Figure 3.4 - The screen of the monitor of the splicer. In the first figure it is possible to see the profiles of two fibers to be bonded. In the second you can see the signal loss of the junction reported by the displacer

Even though you follow all these steps, the junctions often have to be remade, because the error is an event very probable due to the size of the core of the fiber.
Furthermore you will see that the junctions are a very big source of problems.

3.2 Samples

The sample is an aluminum bar. More samples have been used during the tests, their sizes are 500 x 1.9 x 25 mm.

Figure 3.5 - Section of the sample

Furthermore, the samples have different number of fiber and different number of Bragg Grating per fiber.

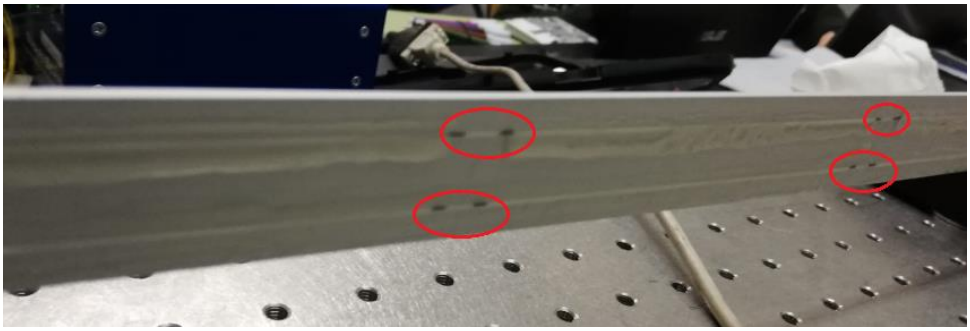

Figure 3.6 - In the picture there is an example of sample with two fibers, and each fiber has two Bragg Gratings

Lastly a sample in composite material has been tested.
This sample has been made by Icarus team, but they did not know the properties of their material. The composite materials are materials made of two or more constituent materials with significantly differences from the individual components. There are usually an element with strengthening action, the fiber, and a spread element called matrix.

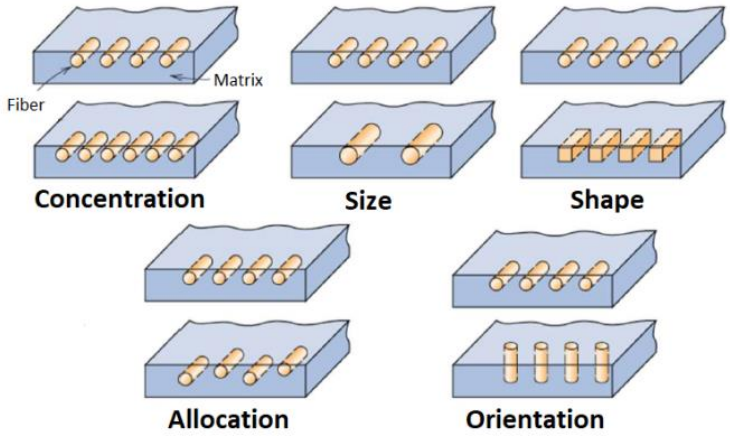

Figure 3.7 - The properties of the composite material are defined by a lot of variables about the coupling of the fibers and the matrix

Hence, not having sufficient data of the material of the new kind of sample, the FEM analysis with Patran-Nastran cannot be implemented. Then to control the output of the FBG a strain gauge is used. Moreover, the shape of this sample is irregular and it may be difficult to model, but also this problem is passed with strain gauge.

Figure 3.8 - Sample in composite

3.3 Adhesive Araldite 2011

The adhesive used to paste the fiber on the samples is Araldite 2011. It is a bicomponent adhesive obtained from the union of a resin with an hardener. It has good resistance to static and dynamic loads and it polymerises at ambient temperature. To apply the adhesive, in every case of study of the teams, you need to clean very well the surface and the fiber to glue.
Then the glue is placed with an applicator with a mixer on the top.

The cleaning and the mixing of the adhesive are the two fundamental steps to make an optimal gluing.

Figure 3.9 - Mixer and applicator of the adhesive

3.4 Test Bench and Breadboard

The tests are strongly influenced by external disturbances. The measurements could be distorted just by the vibration produced by a bus passing on the street outdoor.
So you need two layers: the first is an heavy breadboard with a very big mass and a damping system to suppress the high frequencies.

Figure 3.10 - First layer: it is a big and heavy table with dampers

The second layer is a smaller breadboard with threaded holes to fix the tools and the samples.

The threaded holes are M6, with 25mm of wheelbase between themselves.

Figure 3.11 - Second layer, the smaller breadboard where samples and tools will be fixed

3.5 Faulhaber MCDC2805

A micromotor has been used to move the tip of the sample. It is a Faulhaber micromotor 2805.

Figure 3.12 - Micromotor Faulhaber

Table 1 - Main features of the Faulhaber micromotor

Parameters	Values
Voltage	12 V
No-load speed	7800 min^{-1}
No-load current	14 mA
Thermal limit current	520 mA
Max current	1 A
Encoder lines per revolution	512

The micromotor is associated to the micropositioner with an adaptor.

Table 2 - Main features of the planetary gearhead

Parameters	Values
Torque	0.7 nm
Number of stages	5
Transmission ratio	592:1

The controller communicates with the computer through a serial communication RS-232.

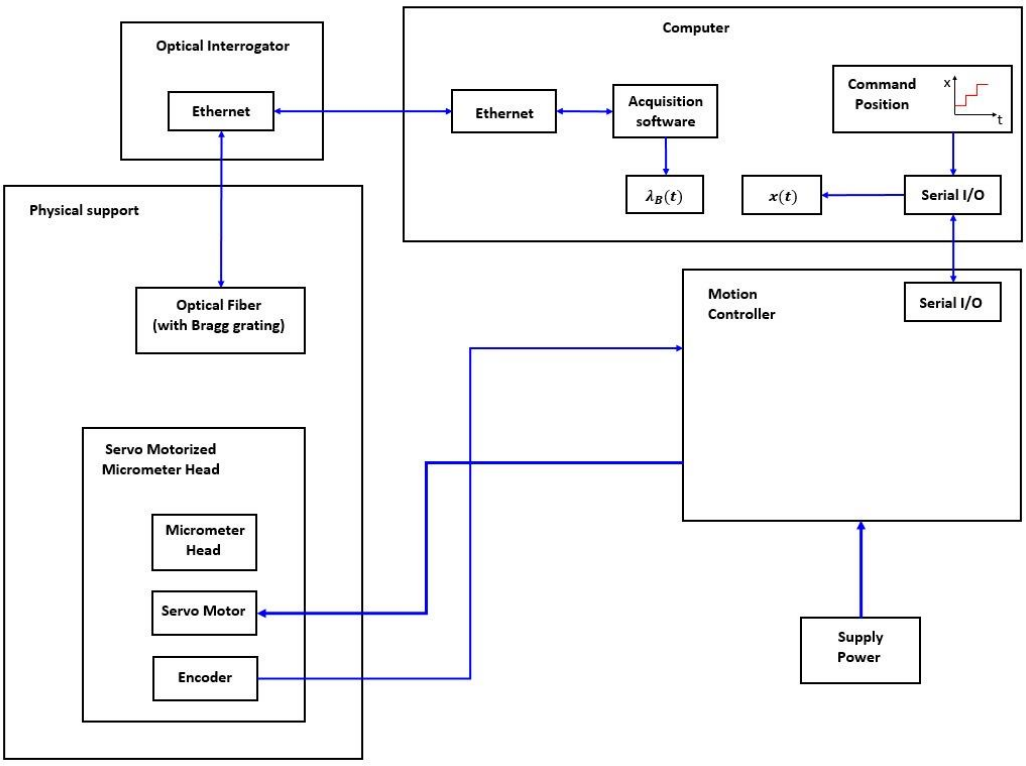

Figure 3.13 - Functional block diagram

Table 3 - Main features of the power supply

Parameters	Values
AC input voltage	110/220 V 1.1 V 50/60 Hz
DC output voltage	24 V
Output current	10 A
Power	240 W

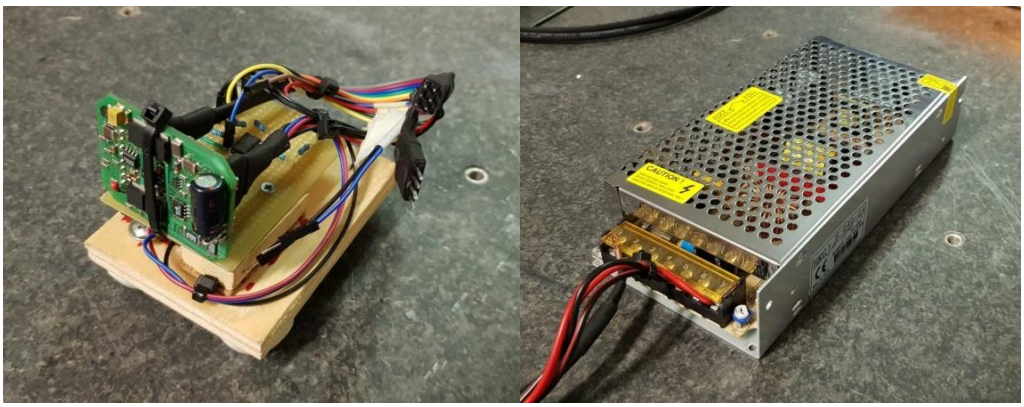

Figure 3.14 - Picture with electronic of the motion controller and the supply power

3.6 Micropositioner

The micropositioner is a device which transforms the rotational motion of the micromotor in a translation motion. Then, with a rigid body, the micropositioner is applied on the tip of the sample.

Table 4 - Main features of the micropositioner

Stroke [mm]	Speed [mm/s]	Resolution [μm]	Accuracy [μm]
25	0.11	0.2	$< \pm 3$

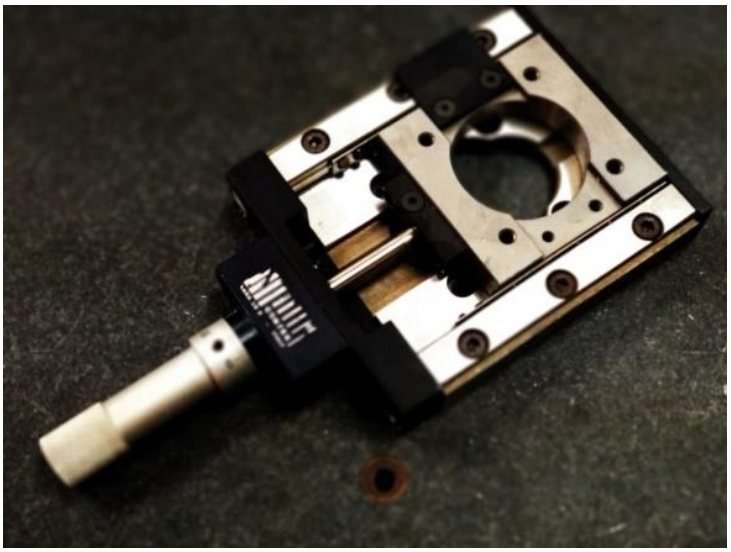

Figure 3.15 - Micropositioner

3.7 Supports

Various supports have been designed to hold the micromotor, the micropositioner and the sample. All of them are planned on Solidworks and they are made with additive manufacturing.

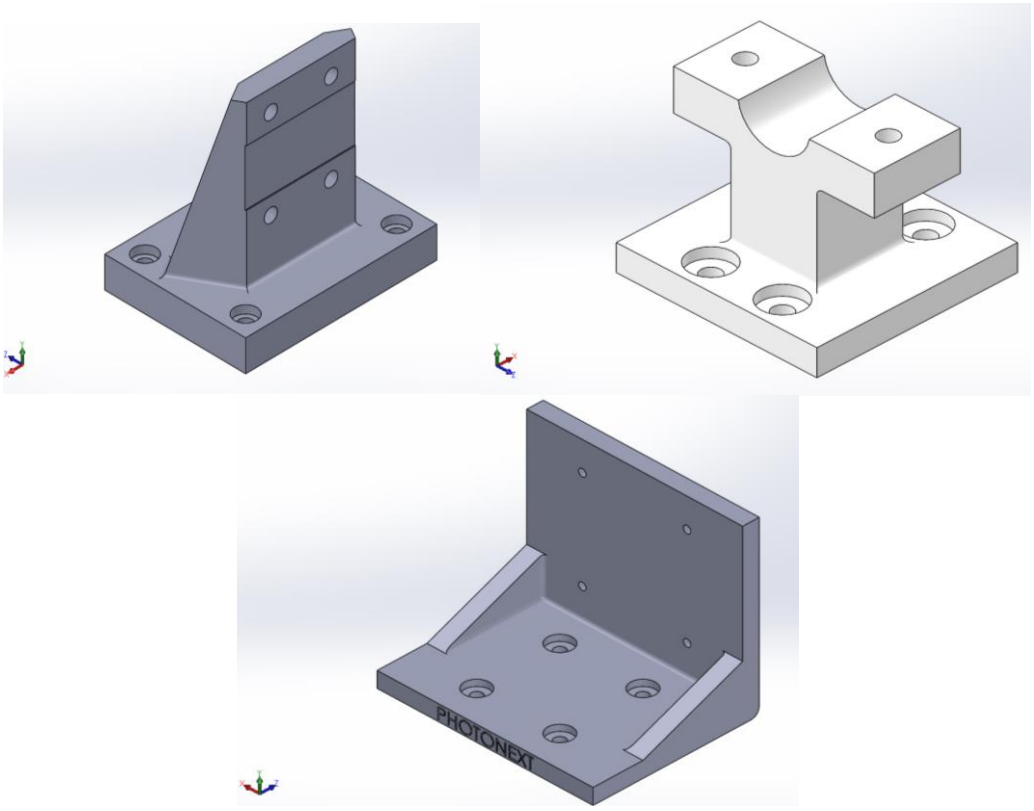

Figure 3.16 - The cad projects of our supports of sample, Faulhaber micromotor and micropositioner in order of time-of-day

The supports of the micromotor and of the micropositioner are efficient, but the support of the samples become deformed when a torque is applied. So a support in steel has been preferred to hold the samples.

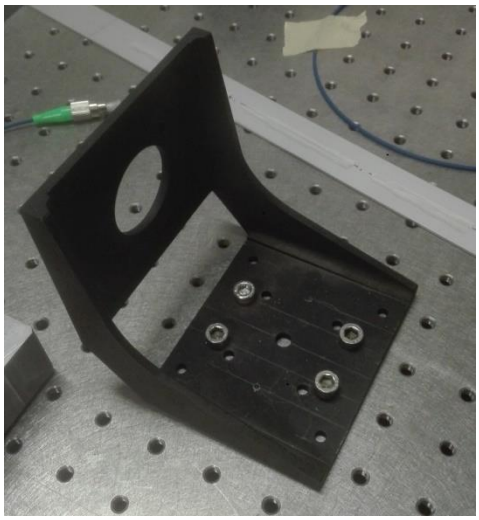

Figure 3.17 - Iron support

3.8 Interrogator

The interrogator is the device which sends the signal of light to the fiber and it also receives and reads the signal reflected by Bragg Grating

Figure 3.18 - Interrogator

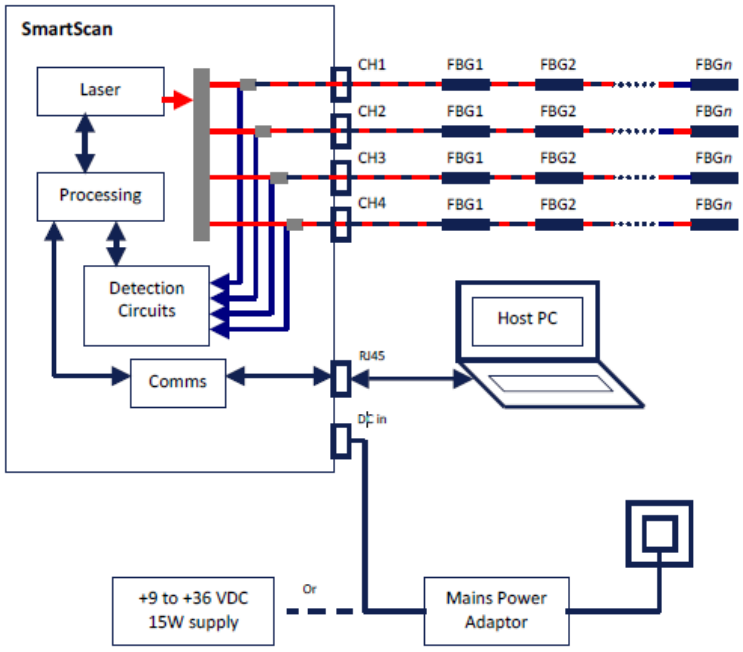

Figure 3.19 - SmartScan system diagram [6]

Table 5 - Datasheet of interrogator [6]

Parameters	Values
Wavelength	1528 - 1568 nm
Number of optical channels	1, 2, 3 or 4
Maximum number of sensors per channel	16
Bragg Grating full width half maximum	0.2 nm
Scan frequency	2.5 kHz
Repeatability	< 1 nm
Wavelength stability	$< \pm 5$ pm (over operating temperature range)
Dynamic range	27 dB
Operating temperature	-10° to 50° C
Input voltage	9 to 36 V DC or 100 to 240 V AC
Power consummation	typ 7.5 W, max 10 W

There is not a specify electronic block diagram of the Interrogator, [7] however you know that a fiber optic link includes:

- Light source and a receiver. For the light sources LED (light emitted diode), SLED (superluminescent LED) or LD (laser diode) are used. For the receiver a photodiode is used. It is a semiconductor P-N junction used to convert light into electrical current.
- Connectors, discussed above in the section regarding the junction of our FBGs.
- Isolator to protect the source from back-reflected light. It is a passive device that allows the optical signal to pass only in one direction, like a non-return valve.
- Coupler or a circulator to route properly the optical signal from the source to the sensor and from the sensor to the receiver. Its purpose is similar to the isolator, but it works with three or more ports.

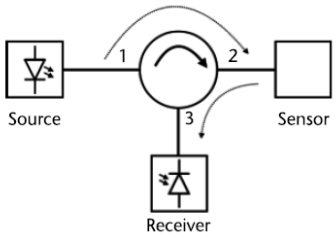

Figure 3.20 - Schematic representation of the use of a circulator to interrogate a sensor working in reflection [7]

- Filters to allow passing or reflecting only specific wavelengths
- Polarizers to select only specific light polarization states. A polarizer is a two-port device that allows light waves with a specific polarization only pass.

3.9 Strain Gauge Aihasd 5PCS BF350

[8] Strain gauges are used to measure directly the strain on a surface. They consist of a long arrow metal conductor mounted on a polyimide film. Hence, the strain gauge is glued on the surface in the point where you want to make the analysis of the strains. If the surface flexes the device will follow the movements of the elements and the arrow will modify its length. The change of length takes to a proportional variation of the resistance, measuring this variation the strain will be found.

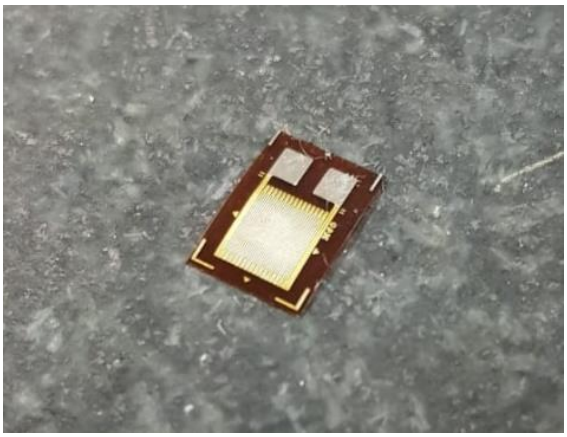

Figure 3.21 - Strain Gauge Aihasd 5PCS BF350

$$R = \rho \frac{L}{A} \tag{9}$$

Where R is the resistance, ρ is the electrical resistivity, L is the length and A is the cross section area.

$$lnR = ln\rho + lnL - lnA \quad \rightarrow \quad \frac{dR}{R} = \frac{d\rho}{\rho} + \frac{dL}{L} - \frac{dA}{A} \tag{10}$$

The cross section of the area is given by the width (w) and the height (h), since you have:

$$\frac{dA}{A} = \frac{wdh + hdw}{wh} = \frac{dh}{h} + \frac{dw}{w} \tag{11}$$

The poison ratio is defined by:

$$v = \frac{\varepsilon_{trasverse}}{\varepsilon_{axial}} = -\frac{\Delta D/D}{\Delta L/L} \tag{12}$$

Considering

$$\frac{dh}{h} = -v\frac{dL}{L} \qquad\qquad \frac{dw}{w} = -v\frac{dL}{L} \tag{13}$$

which makes:

$$\frac{dA}{A} = -2v\frac{dL}{L} = -2v\varepsilon_{axial} \tag{14}$$

Substituting the equation (14) back into equation (10):

$$\frac{dR}{R} = \varepsilon_{axial}\ 1 + 2v\ + \frac{d\rho}{\rho} \quad \rightarrow \quad \frac{dR}{R}\frac{1}{\varepsilon_{axial}} = \ 1 + 2v\ + \frac{d\rho}{\rho}\frac{1}{\varepsilon_{axial}} \tag{15}$$

Note the elements 1 and $2v$, on the right side, represent the change in resistance due to the increased length and decreased diameter of the conductor. The last term represents the piezoresistive effect of the material, that is the change of resistivity of the material with strain.
The relative sensitivity of the device is given by γ, the gauge factor:

$$\gamma = \frac{\Delta R/R}{\varepsilon_{axial}} \tag{16}$$

The Gauge factor is a characteristic parameter of the strain gauge, so, to make the measure, you capture the ΔR and the strain is obtained with:

$$\varepsilon_{axial} = \frac{\Delta R/R}{\gamma} \tag{17}$$

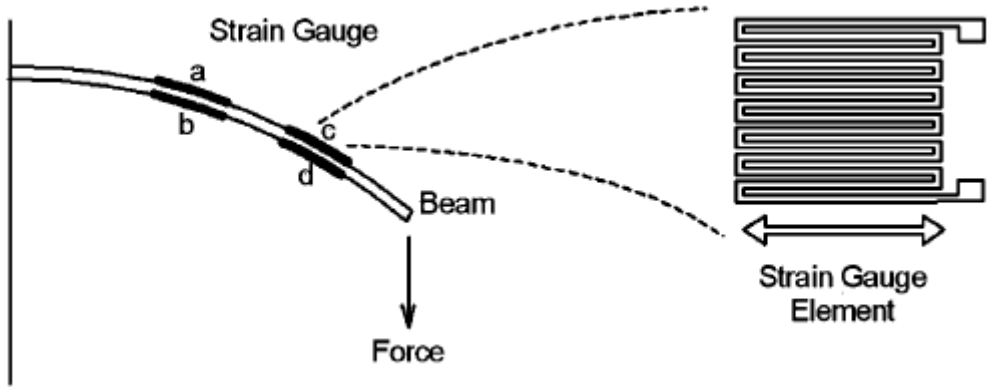

Figure 3.22 - Example of operation of the strain gauge [8]

The value of ΔR is found with a resistive partitor.

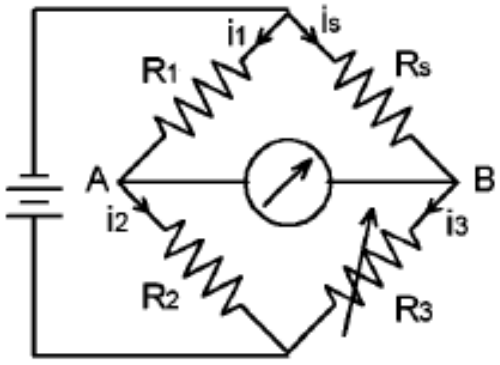

Figure 3.23 - Static balanced bridge circuit, with R_s that is the resistance of strain gauge

The capture of the values is effected automatically by the instrumentation of the department, that gives back the microstrains already transformed. The strain gauges used for the work have the following features:

Table 6 - Main features of the strain gauge

Parameters	Values
Typical resistance	350 Ω
Gauge factor	2.00 - 2.20
Sizes	7.5x4 mm

4 Software

4.1 SmartSoftSSI v3.2.0

The interrogator uses SmartSoftSSI to import data into the computer.
In the main screen you can see the graph in real time with the responses of the fiber. At the top left it is possible to choose how many fibers analyzing, then it is also possible telling to the software how many Bragg gratings there are on each fiber. The interrogator is able to analyze until 64 gratings. In this screen it is also possible to specify other parameters like the frequency of sampling and the minimum peak value detectable as percentage of signal.

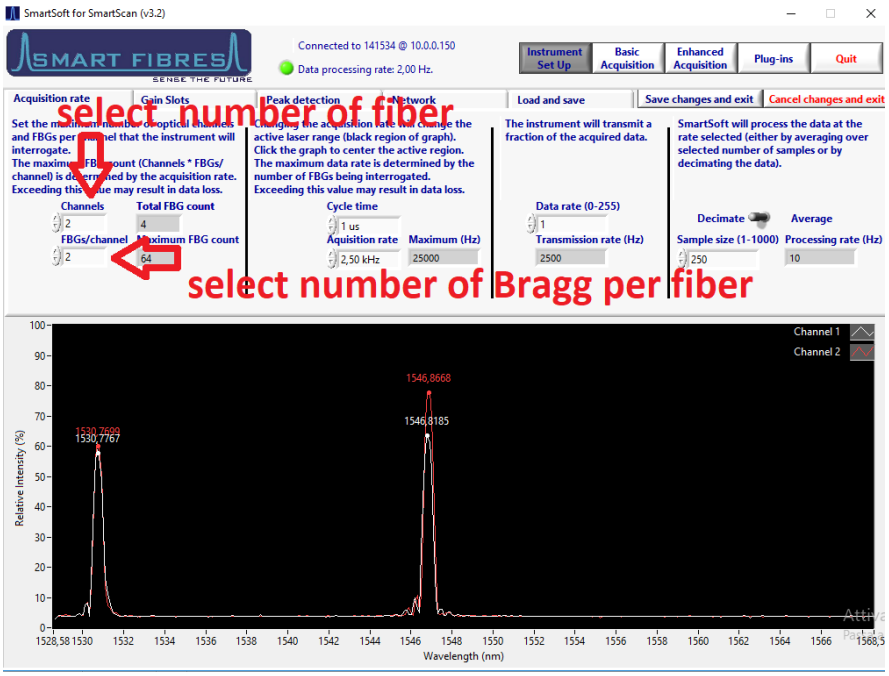

Figure 4.1 - Main screen of SmartSoftSSI. In this example there are two fibers with two Bragg Gratings for each fiber, Fiber #1 is the white curve and Fiber #2 is the red curve

To start the analysis of the FBG you need to open the window “basic acquisition”, naming the new file and starting the software. When the analysis will be completed the software creates a file .log in the previously specified folder.

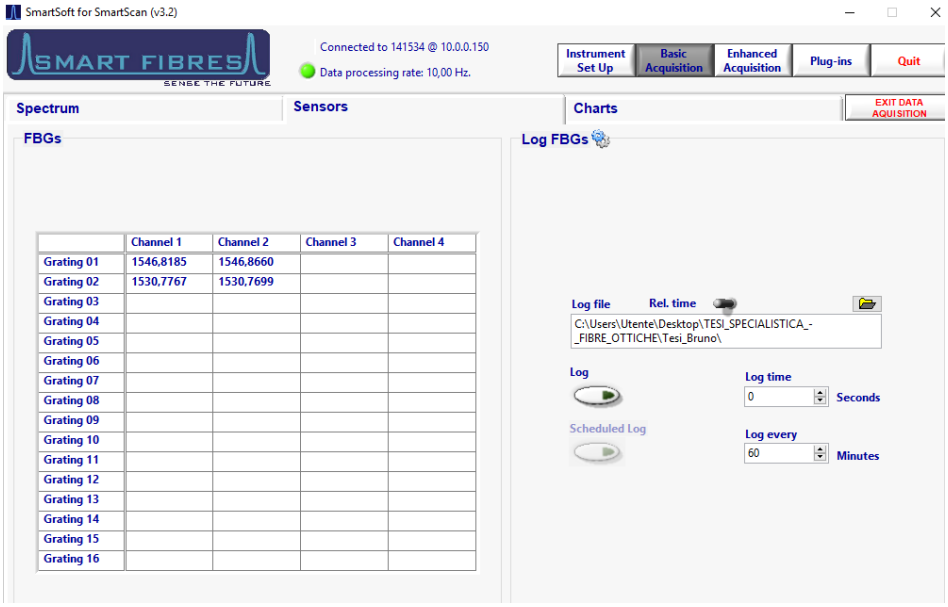

Figure 4.2 - The screen for the basic acquisition. It the same example with two fibers and two Bragg grantings

19-01-14_L4 - Blocco note

File Modifica Formato Visualizza ?

```
Start Time (UTC) = 1547479681,546064
Time interval = 100000 us

Time     Ch01Gr01         Ch01Gr02         Ch02Gr01         Ch02Gr02
         Wavelength (nm) Wavelength (nm) Wavelength (nm) Wavelength (nm)
0,000000         1546,8551        1530,7660        1546,8037        1530,7737
0,100000         1546,8559        1530,7668        1546,8045        1530,7752
0,200000         1546,8551        1530,7660        1546,8037        1530,7752
0,300000         1546,8559        1530,7660        1546,8045        1530,7744
0,400000         1546,8559        1530,7645        1546,8045        1530,7737
0,500000         1546,8551        1530,7660        1546,8037        1530,7744
0,600000         1546,8559        1530,7653        1546,8052        1530,7744
0,700000         1546,8559        1530,7668        1546,8060        1530,7752
0,800000         1546,8559        1530,7653        1546,8045        1530,7744
0,900000         1546,8559        1530,7653        1546,8052        1530,7737
1,000000         1546,8551        1530,7653        1546,8029        1530,7744
1,100000         1546,8551        1530,7660        1546,8037        1530,7752
1,200000         1546,8559        1530,7660        1546,8037        1530,7752
1,300000         1546,8551        1530,7653        1546,8045        1530,7737
1,400000         1546,8559        1530,7660        1546,8052        1530,7752
```

Figure 4.3 - An example of the output file of the SmartSoftSSI. This output presents the analyse of two fibers and each fiber has two Bragg Gratings (Ch = channel, Br = Bragg grating)

The output file includes as many columns as the number of Bragg gratings which have been analyzed by the SmartSoftSSI.

The first column has the time values. In the previous imagine, for example, there are two Bragg gratings in the Fiber #1 (Ch1 Br1 and Ch1 Br2) and other two on the Fiber #2 (Ch2 Br1 and Ch2 Br2).

4.2 Matlab

The SmartSoftSSI returns values extremely variable, like these in the picture, with a rate of 10Hz. Hence, a package of post processing is needed.

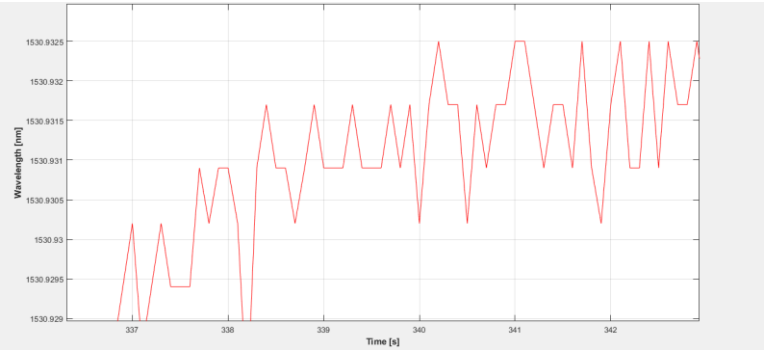

Figure 4.4 - Example of values in output from the software

Matlab has been chosen to implement this.

4.2.1 C2_Post_processing_gradient

At first the data are acquired in a matrix, secondly they have been filtered and they are transformed in a first order. This process generates a little delay in the signal, but it is irrelevant for the purpose of the thesis.
Then, the values we are focusing on are the results of the fiber in correspondence of the steps, when the tip of sample is stopped, so the Matlab script has to extract the mean of the steps.
Hence, the Matlab script returns as output the following data:

- a table with mean of the wavelength of the steps
- a table with the confidence interval of the steps
- a table with the mean microstrain ϵ of each step
- some graphs of the performance of the wavelength of every FBG

In the following imagine you can see the effect of script on the results,

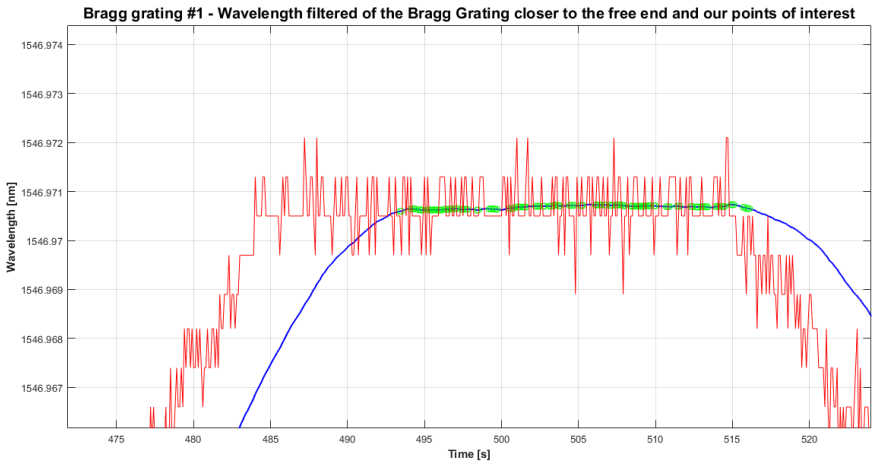

Figure 4.5 - Processing of the values of wavelength and extraction of the mean of the step

In the figure above there are three elements: the red line is the signal in output from interrogator, the blue line is the curve filtered and it is slightly delayed. Lastly the green points are the constant values, their sum gives the mean of that step.
This script has been used also to analyse the output given by the strain gauge.

4.2.2 E1_Confrontatore

This script takes the theorist values of ϵ, given by Nastran - Patran, and it compares them with the results given by FBG.
In output it provides:

- a table with the percentage of error of the strain of the fiber compared with the Nastran - Patran output for each step
- a graph of the strains of FBG and Nastran - Patran in ordinate and the steps in abscissa.

4.3 MSC Nastran 2018 and Patran 2018

To validate the FBG you need an analysis FEM, already tested, which returns the strains of the points where the FBGs are glued.

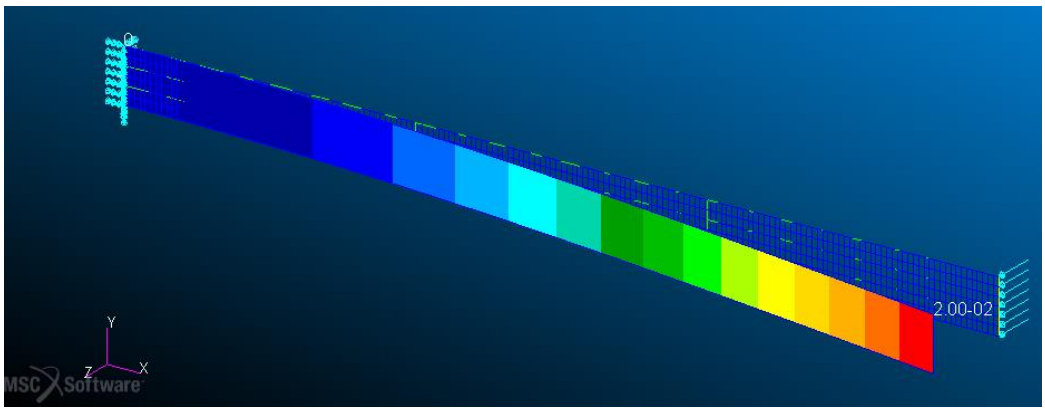

Figure 4.6 - Scheme on Patran of our sample with 20mm of deformation at the tip

The software is able to show the strains for each quad mesh, but also to generate an append file with the strains of elements previously selected.

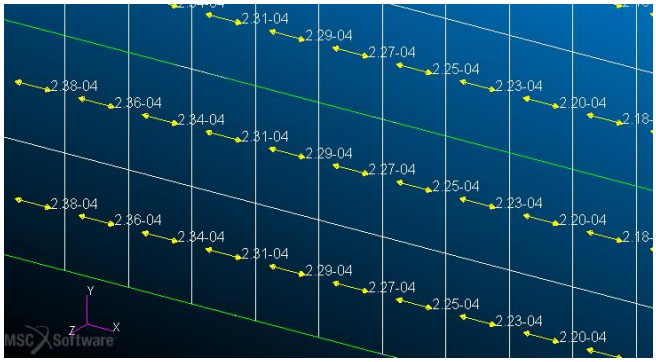

Figure 4.7 - Strains shown visually on the monitor

5 Tests and Results

5.1 2F_2B test - Sample with two Fibers and two Bragg Gratings for each Fiber

Before testing every FBG, it is necessary to prove the gluing of the fiber to the sample.
In order to achieve it, the sample has been deformed with a deformation of 25mm at the tip; it has been fixed with this configuration for a long time (from 20 to 40 minutes). Then, the interrogator records during the test. Once completed the test you control the signal of the FBG: if the loss of the signal is in the order of thousandths of nanometer the gluing is valid.
In this test the sample has two fibers and each fiber has two Bragg Gratings. The purpose of this test is, in particular, to seek any difference between Fiber #1, with continuous gluing, and Fiber #2, with spot-gluing.

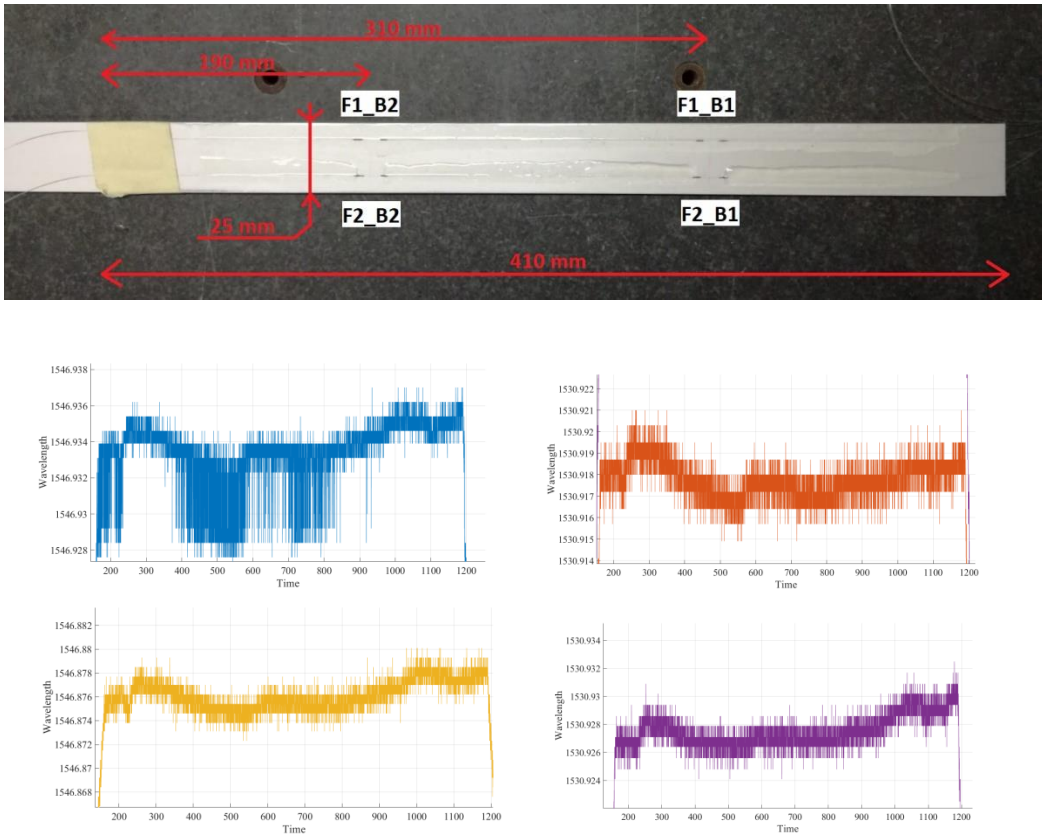

Figure 5.1 - 2F_2B sample and gluing control

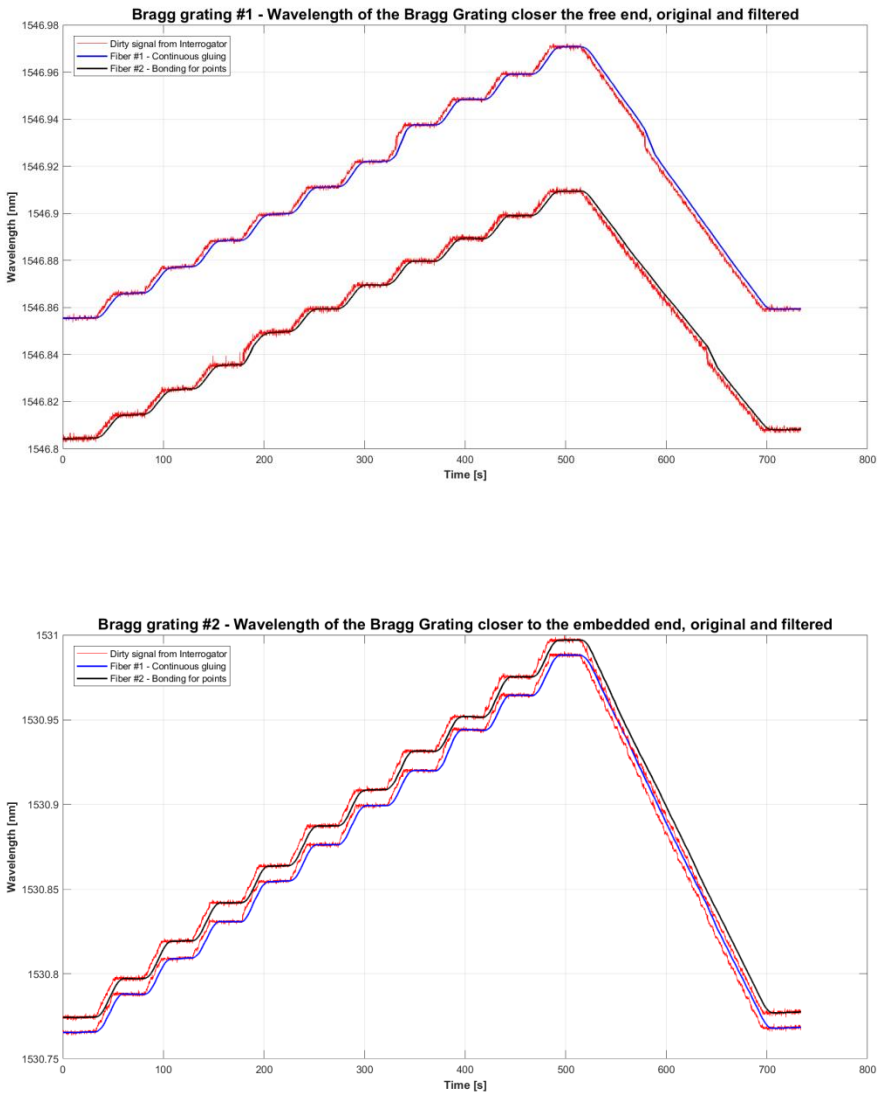

Figure 5.2 - In the two graphs above there are the signals of the FBGs original, from Bragg#1 the first and from Bragg#2 the second. Then there are also their filtered values

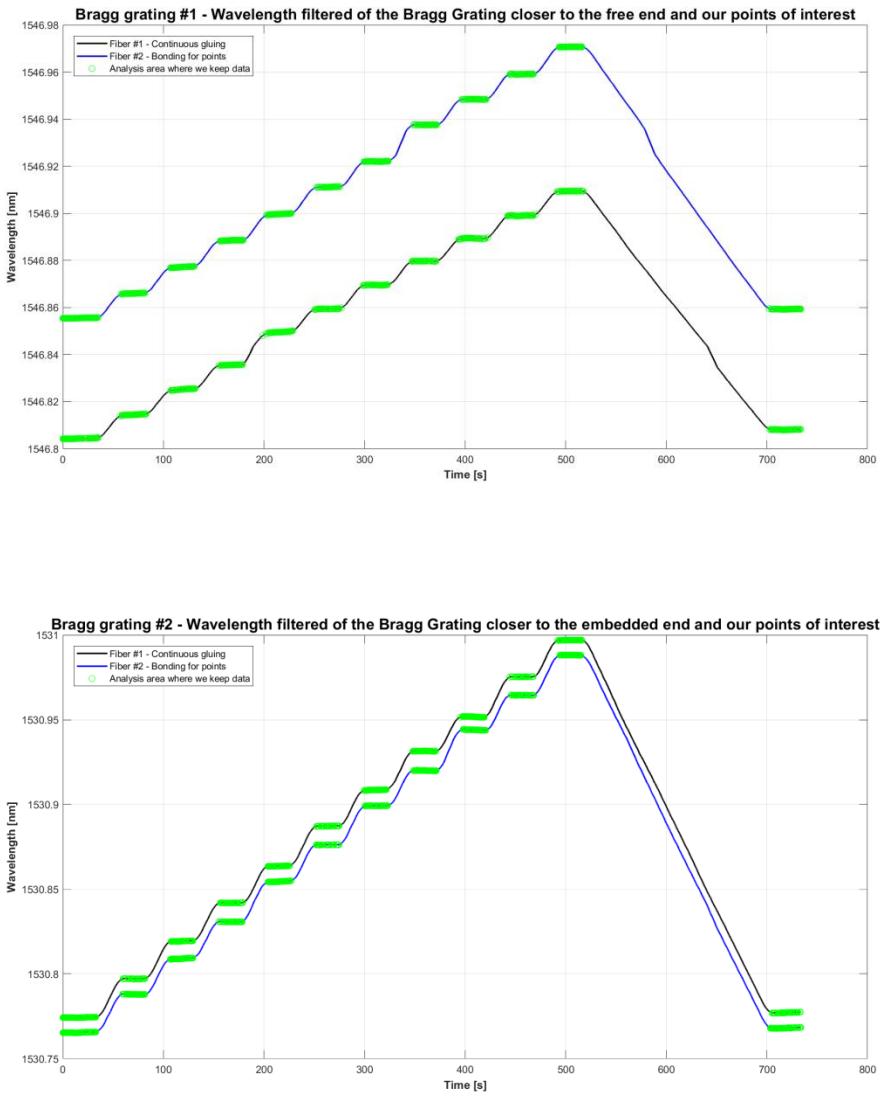

Figure 5.3 - In the two graphs above there are the filtered signals of the FBGs with the areas of interest. These values are highlighted in green in the graphs

Table 7 - Mean and Confidence interval of the steps of the F2_B2 sample, made on the 14th January 2019

	F1 - B1		F1 - B2		F2 - B1		F2 - B2	
Steps [mm]	Mean [nm]	Confidence interval at 95% [nm]	Mean [nm]	Confidence interval at 95% [nm]	Mean [nm]	Confidence interval at 95% [nm]	Mean [nm]	Confidence interval at 95% [nm]
0	1546,85552	1546,85551	1530,76553	1530,76552	1546,80436	1546,80434	1530,77440	1530,77439
		1546,85554		1530,76555		1546,80438		1530,77441
2	1546,86602	1546,86600	1530,78808	1530,78806	1546,81447	1546,81444	1530,79724	1530,79722
		1546,86604		1530,78810		1546,81450		1530,79725
4	1546,87715	1546,87711	1530,80913	1530,80908	1546,82524	1546,82519	1530,81939	1530,81937
		1546,87719		1530,80917		1546,82529		1530,81942
6	1546,88849	1546,88848	1530,83083	1530,83082	1546,83560	1546,83558	1530,84197	1530,84196
		1546,88851		1530,83084		1546,83562		1530,84198
8	1546,89967	1546,89964	1530,85457	1530,85453	1546,84952	1546,84947	1530,86370	1530,86367
		1546,89969		1530,85461		1546,84957		1530,86372
10	1546,91117	1546,91116	1530,87621	1530,87619	1546,85942	1546,85940	1530,88728	1530,88726
		1546,91119		1530,87622		1546,85944		1530,88730
12	1546,92203	1546,92202	1530,89925	1530,89924	1546,86955	1546,86953	1530,90859	1530,90856
		1546,92204		1530,89926		1546,86956		1530,90861
14	1546,93758	1546,93758	1530,92010	1530,92008	1546,87970	1546,87969	1530,93152	1530,93151
		1546,93759		1530,92011		1546,87971		1530,93153
16	1546,94844	1546,94843	1530,94410	1530,94407	1546,88936	1546,88934	1530,95176	1530,95173
		1546,94845		1530,94413		1546,88939		1530,95179
18	1546,95907	1546,95906	1530,96454	1530,96453	1546,89903	1546,89901	1530,97538	1530,97536
		1546,95908		1530,96455		1546,89905		1530,97539
20	1546,97068	1546,97067	1530,98816	1530,98815	1546,90940	1546,90939	1530,99705	1530,99703
		1546,97069		1530,98817		1546,90941		1530,99706

In Table 7 you can see that the 95% of the values of each step is within a very little range (in the order of 0.00001nm!). Hence, the results can be considered plausible and the means of the steps valid.

Table 8 - Microstrains recorded by the FBGs of 2F_2B, made on the 14th January 2019

Displacement imposed to the tip	Strain recorded by the FBG [$\mu\epsilon$]			
	F1 - B1	**F1 - B2**	**F2 - B1**	**F2 - B2**
2 mm	8,696	18,882	8,383	19,127
4 mm	17,921	36,509	17,31	37,68
6 mm	27,326	54,69	25,896	56,591
8 mm	36,586	74,569	37,434	74,786
10 mm	46,123	92,69	45,64	94,541
12 mm	55,12	111,989	54,029	112,384
14 mm	68,009	129,45	62,446	131,587
16 mm	77,008	149,551	70,454	148,541
18 mm	85,82	166,673	78,465	168,32
20 mm	95,442	186,455	87,061	186,47

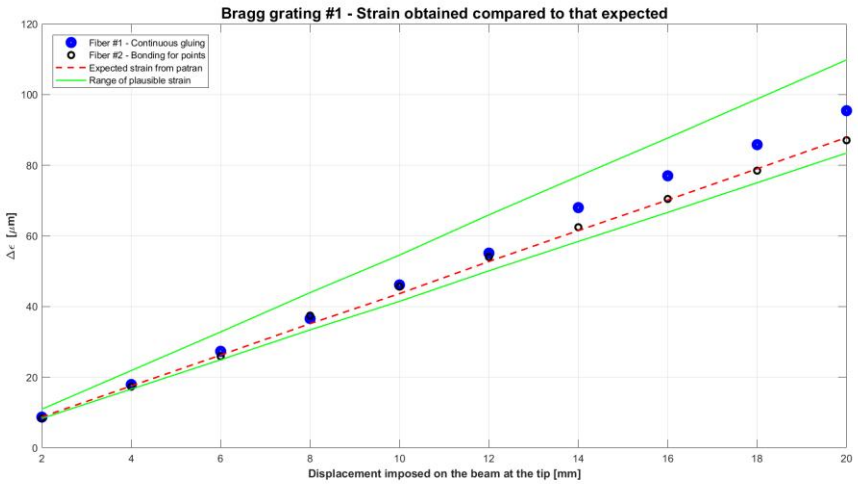

Figure 5.4 - Progress of microstrain, in the Bragg Gratings #1, of the two fibers, by the FBGs of 2F_2B, made on the 14th January 2019. The red line is the expected value of microstrains in output from Nastran - Patran. Instead, the zone between the green lines, is the range of plausible values, it depends on the thickness of the glue used

Table 9 - Percentage error of the Bragg grating #1 respect the values from Nastran - Patran of the sample 2F_2B, made on the 14th January 2019

Error of the Bragg gratings respect values made by Nastran - Patran #1 [%]	
Fiber 1	**Fiber 2**
-0,62	-4,19
2,41	-1,09
4,10	-1,35
4,09	6,50
5,67	4,56
4,49	2,42
10,58	1,54
9,78	0,43
8,63	-0,68
8,64	-0,90

Now the results of the Bragg gratings of the two fibers are submitted.

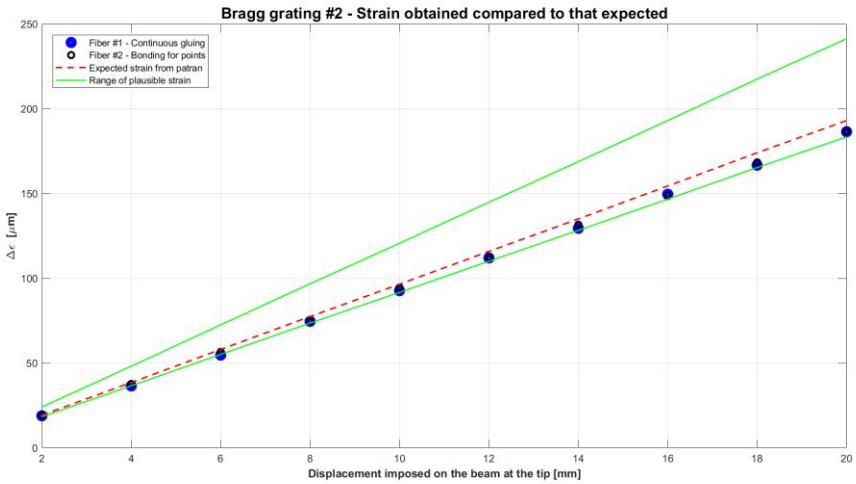

Figure 5.5 - Progress of micro strain, in the Bragg Gratings #2, of the two fibers, by the FBGs of 2F_2B, made on the 14th January 2019. The red line is the expected value of microstrains in output from Nastran - Patran. Instead, the zone between the green lines, is the range of plausible values, it depends on the thickness of the glue used

Table 10 - Percentage error of the Bragg #2 respect the values from Nastran - Patran of the sample 2F_2B, made on the 14th January 2019

Error of the Bragg gratings respect values made by Nastran - Patran #2 [%]	
Fiber 1	**Fiber 2**
-1,91	-0,64
-5,17	-2,13
-5,71	-2,43
-3,66	-3,38
-3,95	-2,03
-3,33	-2,99
-4,11	-2,53
-3,14	-3,79
-4,21	-3,26
-3,39	-3,38

This test is made on the 14th January 2019. Others tests are reported on Appendix A to prove the repeatability of the measurements.

5.1 1F_1B test - Sample with one Fiber and one Bragg Grating, with Alternative Gluing Method

The purpose of the evidence with this FBG is to test a new method of gluing.
The gluing is a big source of problems. If the adhesive is insufficient the FBG is stranded, hence it is subjected to shock. Furthermore, if you apply too much adhesive the fiber will "float" over it; so the glue is led to absorb strain energy and it distorts the results.
This test are made on the 20th February 2019

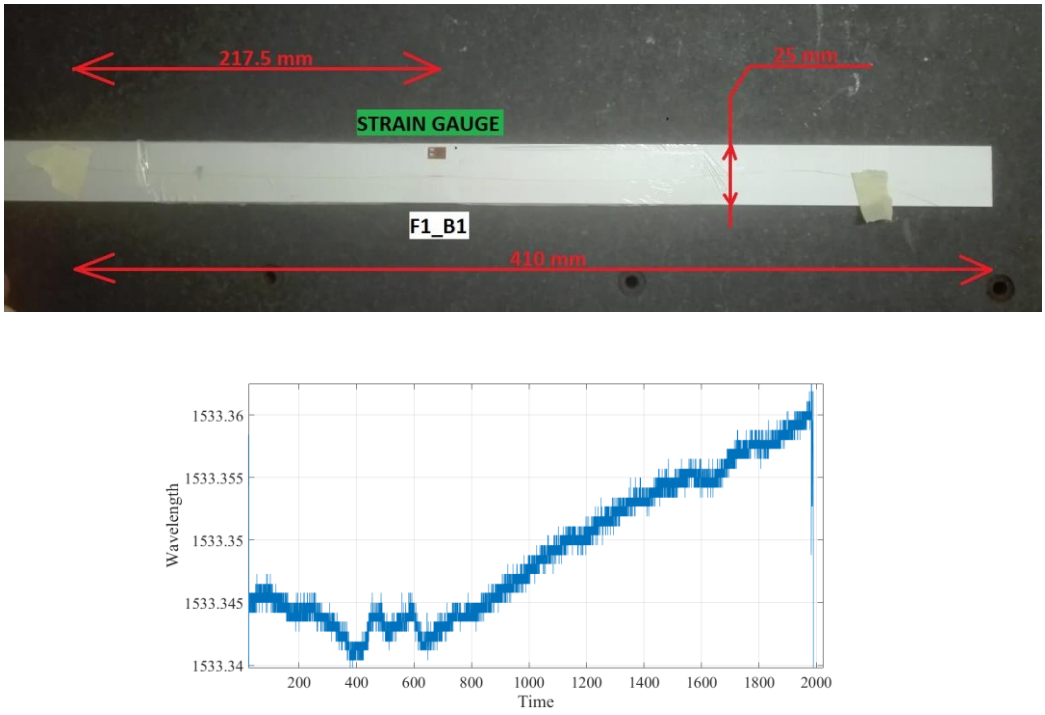

Figure 5.6 - The second sample, 1F_1B, and the graph of the gluing test

It is possible to see that the fiber glued does not loss the signal during the test. The rise of the wavelength is attributable to the adhesive that was polymerizing.

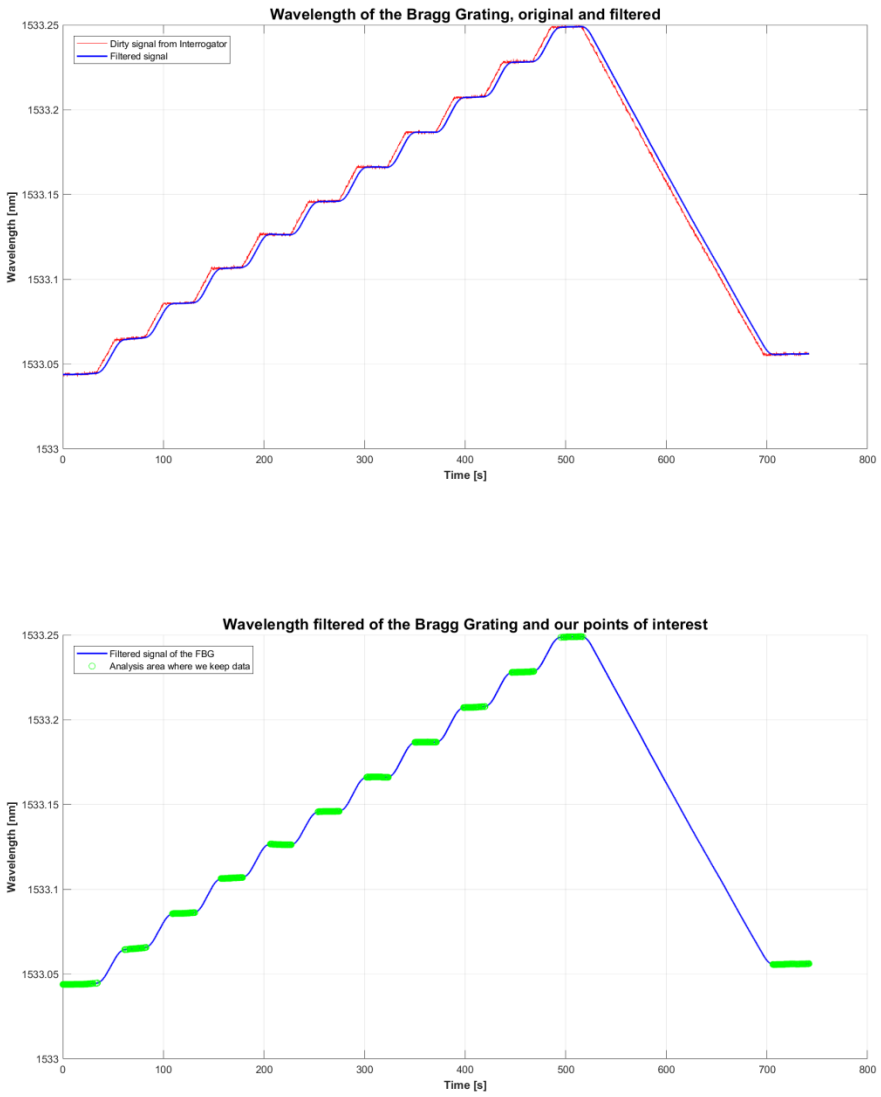

Figure 5.7 - Graphs with original signal from the FBG, the filtered signal and the areas of interest, like in the previous test. This test has been made on the 20th February 2019, on the 1F_1B sample

Table 11 - Mean and Confidence interval of the steps of the F1_B1, made on the 20th February 2019

	F1 - B1	
Steps [mm]	Mean [nm]	Confidence interval at 95% [nm]
2	1533,04396	1533,04394
		1533,04398
4	1533,06502	1533,06496
		1533,06508
6	1533,08581	1533,08578
		1533,08584
8	1533,10659	1533,10656
		1533,10663
10	1533,12634	1533,12632
		1533,12636
12	1533,14588	1533,14586
		1533,14589
14	1533,16621	1533,16620
		1533,16622
16	1533,18676	1533,18675
		1533,18677
18	1533,20741	1533,20737
		1533,20745
20	1533,22818	1533,22816
		1533,22821

Table 12 - Microstrains recorded by the FBG of the 1F_1B sample made on the 20th February 2019

Displacement imposed to the tip	Strain recorded by the FBG [$\mu\epsilon$]
	F1 - B1
2 mm	17,610
4 mm	34,999
6 mm	52,376
8 mm	68,892
10 mm	85,230
12 mm	102,235
14 mm	119,419
16 mm	136,685
18 mm	154,060
20 mm	171,373

Table 13 - Percentage error of the Bragg grating respect the values from Nastran - Patran of the test of the 1F_1B sample, made on the 20th February 2019

Error of the Bragg gratings respect values made by Nastran - Patran [%]
Fiber 1F-1B
3,59
2,94
3,71
2,06
0,86
0,72
1,03
1,25
1,36
1,40

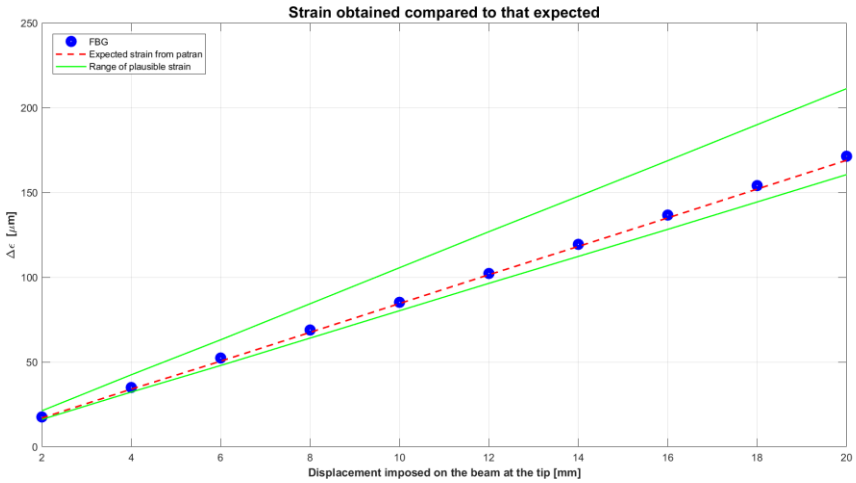

Figure 5.8 - Progress of microstrain, in the Bragg Gratings of the test of 1F_1B sample, made on the 20th February 2019. The red line is the expected value of microstrain in output from Nastran - Patran. Instead, the zone between the green lines, is the range of values plausible, it depends on the thickness of the glue used

As for the previous case, 2F_2B, in the Appendix A there are other cases to prove the repeatability of the measurements.
This sample has been tested also with the strain gauge, after this first step of tests. To compare the two outputs the test made on the 27th February has been chosen, so the glue had time to polymerise properly.

To effect the test two strain gauges have been used: one fixed to measure the strains of the sample, and one free. The purpose of this sensor is to make the measure of deformations caused by variations of temperature. So, after the measuring of the strains of the sample it is possible to consider the compensation of the temperature.

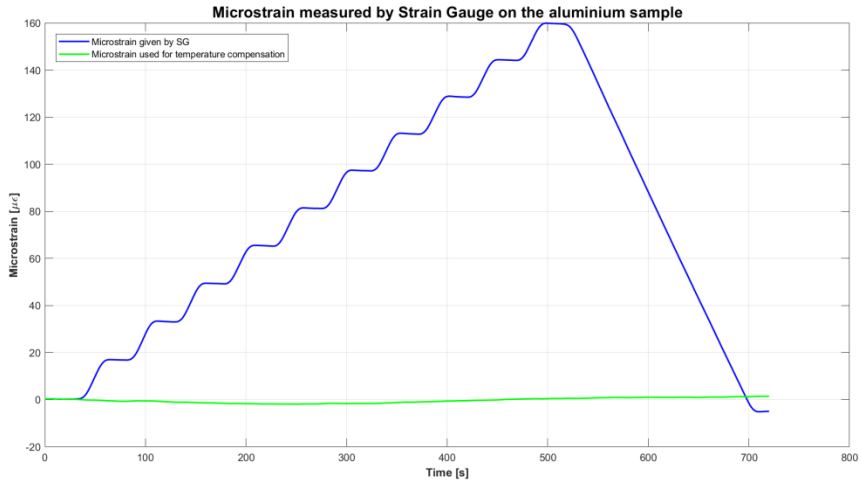

Figure 5.9 - In the graph it is possible to see the strains measured by the strain gauge, the blue line, and the measure of the free strain gauge, with the green line; this will use to do the thermal offset

In the following picture it is possible to see the graph with the microstrains given by the strain gauge illustrated with the black line. It is filtered and thermally compensated. The red line is the average microstrains, measured by the FBG, in the same conditions.

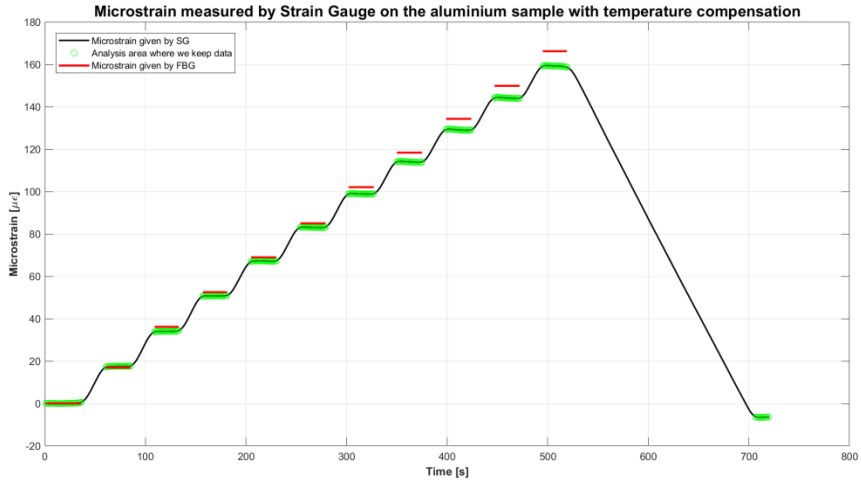

Figure 5.10 - In this picture it is possible to see the measure filtered of the strain gauge in black and the point of interest with the green point. There are also the averages of the steps of the FBG output in the red lines, they are of the test made on the 27th February 2019

More tests has been done, in the following table it is possible to see the error percentage of the FBG compared with the strain gauge output. The test are always made on the 7th March 2019.

Table 14 - The percentage of error of the FBG confronted with the tests done with strain gauge

Displacement imposed to the tip	Error [%]					
	Six tests effected					
2 mm	3,43	1,64	-2,05	2,10	0,90	-6,50
4 mm	-6,19	-8,62	-10,17	-7,61	-8,53	-13,03
6 mm	-3,45	-5,66	-6,69	-5,06	-5,30	-8,31
8 mm	-2,67	-4,35	-5,33	-4,14	-4,63	-6,80
10 mm	-2,27	-3,51	-4,19	-3,38	-3,90	-5,98
12 mm	-3,18	-4,01	-4,40	-3,81	-4,70	-6,24
14 mm	-3,81	-3,88	-4,32	-3,62	-4,62	-5,89
16 mm	-3,98	-3,37	-3,91	-3,20	-4,06	-5,06
18 mm	-3,96	-3,01	-3,40	-2,81	-3,59	-4,69
20 mm	-4,40	-3,27	-3,69	-3,08	-3,97	-4,82

5.2 1F_3B - Sample with a Single Fiber and three Bragg Gratings on it

A sample with a fiber with 3 Bragg Gratings on itself has been tested too. Unfortunately this case has not achieved results. This is due to the links among the Bragg Gratings. The links indeed have a too high signal loss and the interrogator does not read the FBGs downstream of a link, between FBG#1 and FBG#2.

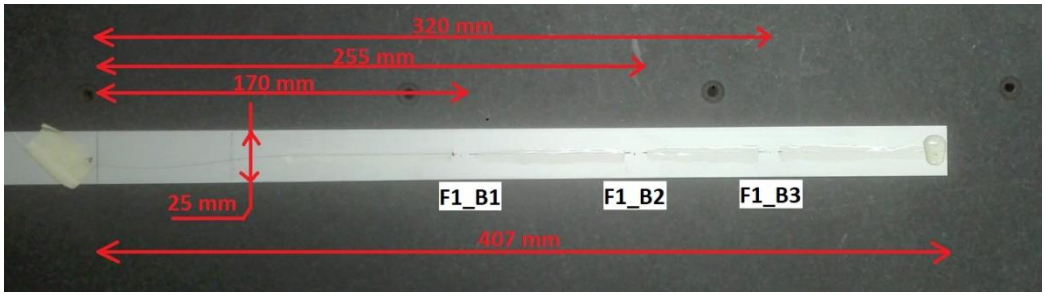

Figure 5.11 - The sample 1F_3B

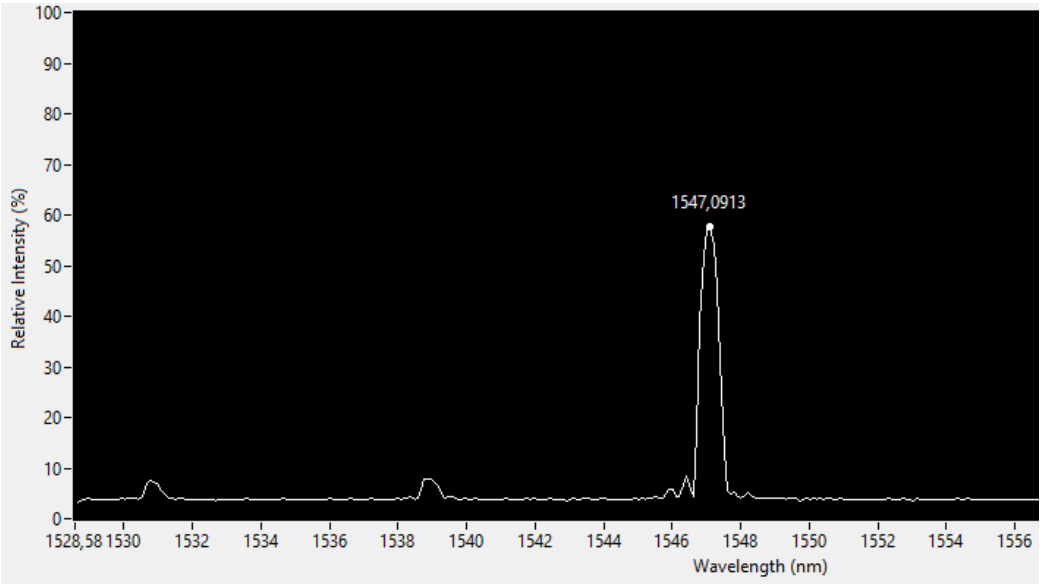

Figure 5.12 - The main screen of the interrogator, it is possible to see the signal of Bragg #1, but the Bragg #2 and #3 are too much low

5.3 1F_1B_composite - Sample in Composite Material

Now you see the results of the FBG on the sample in composite material, compared with these ones of the strain gauge. The test with FBG was made on the 5th of March 2019, instead the test with the strain gauges was made on the 7th of March 2019.

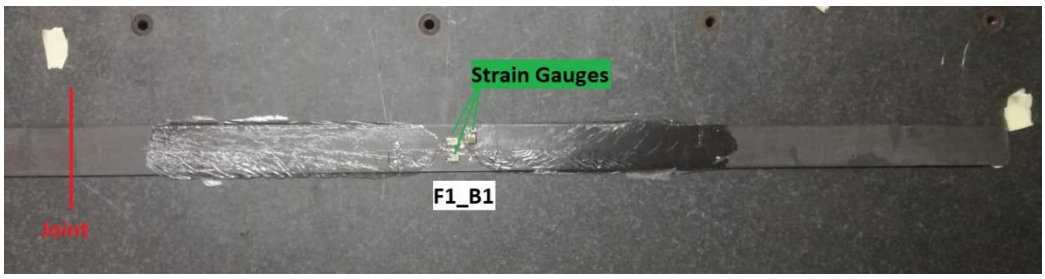

Figure 5.13 - The sample in composite; it is possible to see where the sample is fixed and where the sensors are

The shape of the sample is irregular, but with the strain gauges we do not need to model it in the cad software. So the size of the sample does not matter.
In this case the strain gauges used are: two in the direction of the principal axis of the sample and the strain gauge for the thermal compensation. There is also a strain gauge in the perpendicular direction of the sample, but this will be used for future works.

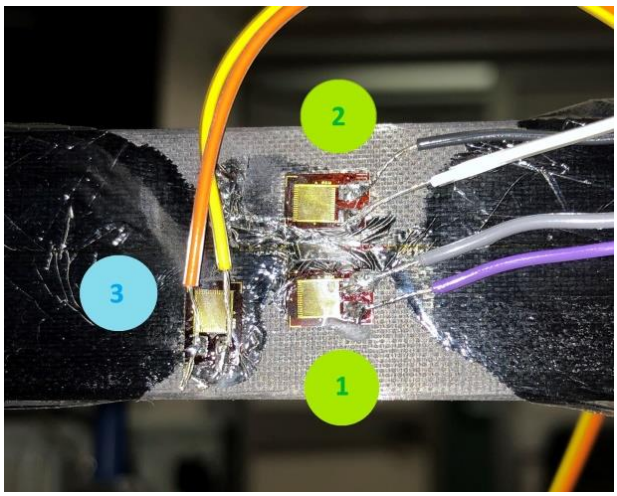

Figure 5.14 - Detail of the sample with the three strain gauges on it. The stain gauges 1 and 2 are for the strain in direction of the principal axis of the sample, and the strain gauge 3 is for the strain in the perpendicular direction

The output obtained is similar to the case of F1_B1 in aluminium, but this time there are two strain gauges for the measure of the strain in the direction of the FBG. So initially, to compare the results, the average between strain gauge 1 and strain gauge 2 is used.

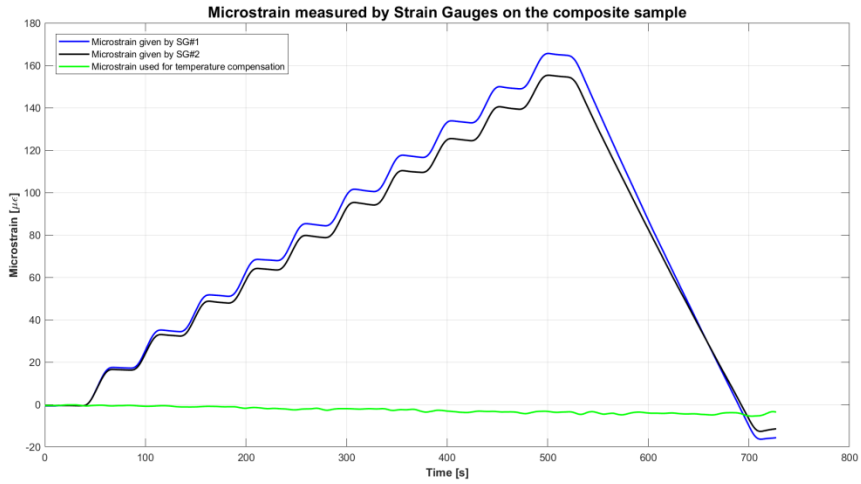

Figure 5.15 - In the graph it is possible to see the strains measured by the strain gauges, the blue line and the black line, and the measure of the free strain gauge; this will use to do the thermal offset

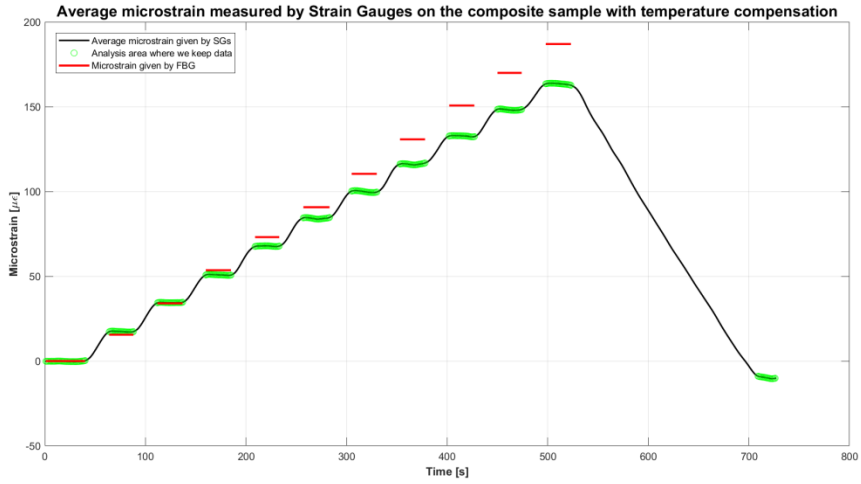

Figure 5.16 - In this picture it is possible to see the measure filtered of the average of the strain gauges, in black, and the point of interest with the green point. The averages of the steps of the FBG output are the red lines

The results of the strains, compared with FBG, are not very good. It is possible to see the percentage error in the Table 15.

Table 15 - The microstrains of the FBG and of the strain gauges with thermal offset and the percentage of error of the FBG confronted with the test done with the average of the strain gauge

Displacement imposed to the tip	Strain recorded [$\mu\epsilon$]			Error [%]
	F1 - B1	SG #1	SG #2	
2 mm	15,536	17,841	16,890	10,53
4 mm	34,023	35,547	33,436	1,36
6 mm	53,581	52,382	49,245	-5,45
8 mm	73,085	69,986	65,609	-7,80
10 mm	90,733	86,983	81,389	-7,78
12 mm	110,412	103,053	96,789	-10,50
14 mm	130,764	119,754	112,507	-12,60
16 mm	150,706	136,910	128,506	-13,56
18 mm	169,954	152,978	143,443	-14,67
20 mm	186,973	168,586	158,382	-14,37

However, you have to take in consideration that the results of strain gauge are strongly influenced by the gluing of themselves. If the photo of the sample with strain gauge is observed carefully, it is possible to see that the strain gauge number 2 is not aligned perfectly with the FBG (Figure 5.17).

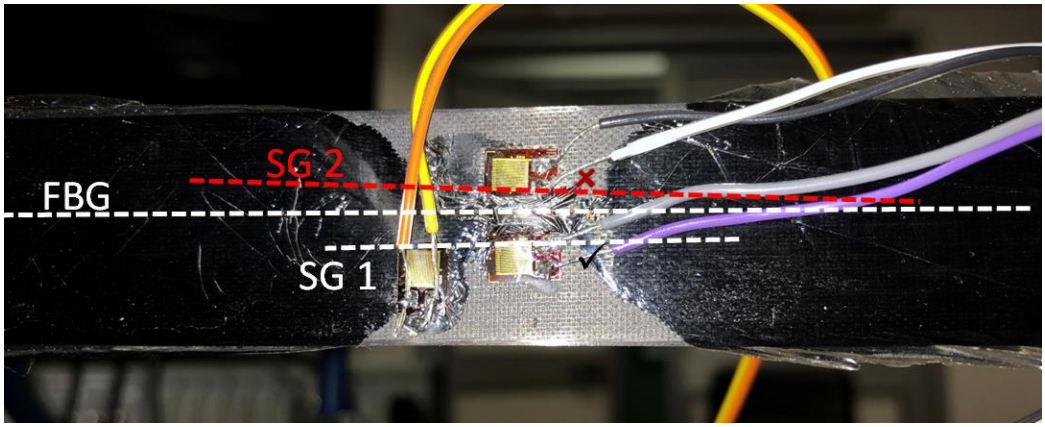

Figure 5.17 - In the picture it is possible to the that the strain gauge 2 is not well aligned with the FBG

If the sensor is not aligned with the FBG it will not measure exactly all the strains which suffers the FBG, and its results will be lower than the others. Indeed the results of SG#2 are the lowest.

With this assumption it is possible to reject the outputs of SG#2. With this correction, and using only SG#1, you see in the following table a perceptible improvement of the error of the measure of the FBG respect to the strain gauge.

Table 16 - Here it is possible to see the percentage of error between the FBG measure and the SG #1, more reliable than SG#2

Displacement imposed to the tip	Error [%]
2 mm	12,92
4 mm	4,29
6 mm	-2,29
8 mm	-4,43
10 mm	-4,31
12 mm	-7,14
14 mm	-9,19
16 mm	-10,08
18 mm	-11,10
20 mm	-10,91

6 Conclusion

At the end of every test, it is possible to define FBG as a valid and innovative remote sensor device. As mentioned above, it benefits of a number of additional advantages, which are the following:

- ✓ **Lightness - Sizes**: FBGs are light and they are very small in size (they seem a human hair). In aerospace, where weight and footprint are very limiting, FBGs could find a huge range of application. For example a FBG, placed on a wing, does not affect the aerodynamics profile.
- ✓ **Insensitive to electromagnetic interference**: the light, passing through the fiber, is not affected by electromagnetic interference. This makes FBGs a robust and reliable measuring instrument.
- ✓ **Potential multi-sensors in the same fiber**: a single fiber could contain multiple Bragg Gratings. Thus obtaining the possibility to make different measurements of different properties, like temperature, pressure, with a single fiber.
- ✓ **Energy independence**: FBG itself does not need external power source, unlike the common electric sensors. Only the Interrogator needs an external power source, then it sends the signal inside the fiber and it grasps the response reflected.

The results in output from the tests have a good response. However, unfortunately, all of them have a little amount of uncertainty. This is because the layer of glue has a thickness and, even though it is subtle, you cannot know where the fiber stays. On the other hand, the CAD project on Patran has a thickness of 2mm. The sample, instead, has a thickness of 1.9mm. Hence, the thickness of glue causes an increase of the measure of the strain.
In the following picture the lateral section of the group is represented. There are the sample and the fiber: it is possible to see that a moment gives a normal stress symmetric (traction on the positive surface and compression on the negative surface).
You see that the fiber has an unknown distance from the surface, this leads to an increase of the stress proportional to the distance.

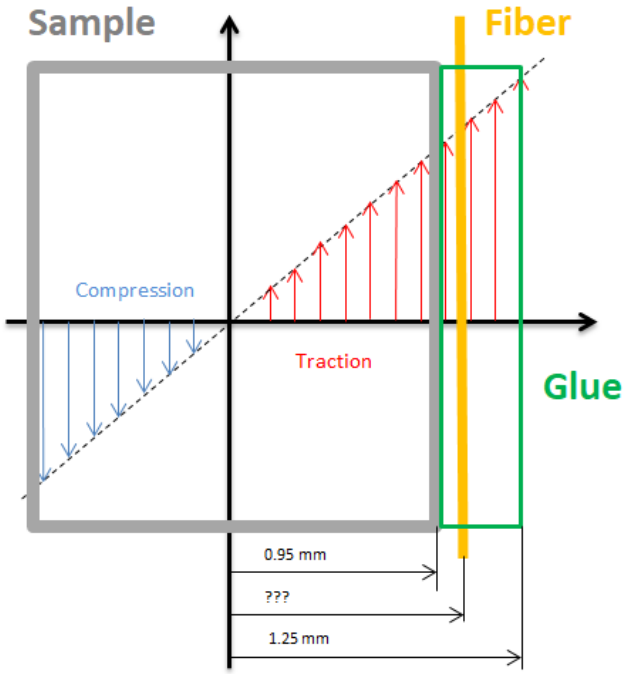

Figure 6.1 - Section of the group sample and fiber glued together

Figure 6.2 - Detail of a graph of the comparison between FBG and Patran-Nastran outputs

In all graphs reported on the thesis you can find:

- Points (black or blue), which are the value of microstrain by the FBG
- Red line, which is the expected value of microstrain given by Patran-Nastran, considering the thickness of the fiber.
- The green lines, which are linearly proportional to the red line. The upper line is the strain in the case the FBG are in the upper position and it is floating over the glue (Figure 6.3 - 1). Instead the downer

line is the case when the fiber is in contact with the sample (Figure 6.3 - 2). This case should be the optimal case.

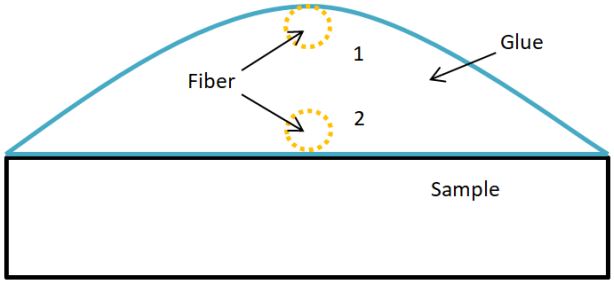

Figure 6.3 - Scheme of frontal section of the group sample and glue, with the possible positions, upper and downer, of the fiber

Hence, the unknown position of the fiber generates an indeterminate value of strain. Supposing to be in the linear field, you can find a range of reliable results. It is possible to see that our values are between the green lines and thus the results are valid.
At the end, the FEM results validate the FBGs and the verification with the strain gauges allows us to declare definitively and categorically the FBGs as valid remote sensors.

During the work, in addition to the problem of the unknown position of the fiber, other problems have arisen:

- **Weakness**: the fiber optics are very fragile especially by shear stress. During the progress of the thesis a lot of fiber optics have been broken, with FBG on it.
- **Connection of the fiber, with FBG, with other fibers or collectors:** the Bragg Gratings used for the work were one per fiber, then, if the test needed it, more FBGs were connected. If the connection was not made in the optimal way, the interrogator recorded a loss of signal. In the test with 1F_3B this event occurred.

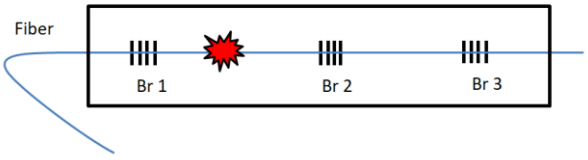

Figure 6.4 - Fiber 1F_3B with a damage between Br1 and Br2

Infact the joint between Br1 and Br2 is not perfect: the cores are not perfectly aligned each other. So the interrogator does not see the Bragg Gratings after the joint (Figure 1F_3B - Sample with a Single Fiber and three Bragg Gratings on it) and it acquires peaks of noise generated by the first Bragg.
Also in the test with 2F_2B it is possible to see a loss of signal:

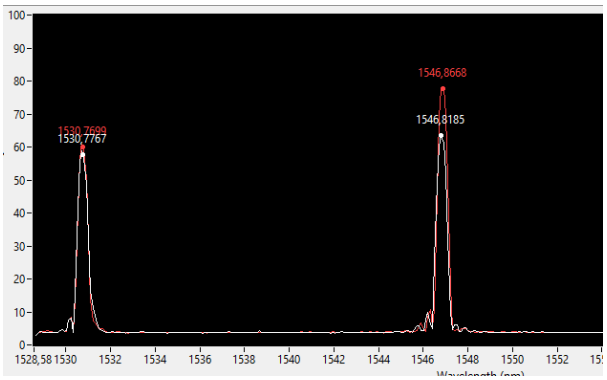

Figure 6.5 - Wavelengths of the fiber test 2F_2B

The red curves (Fiber #1) have different heights. This means there is a little signal loss between two FBG, in any case they are detectable. Instead the white curves (Fiber #2) have the same height, but they are lower than the others. It means that the loss signal is in the joint that links FBGs with the collector.
Unfortunately a low number of FBGs have been used and they are not sufficient to create an adequate statistical basis. In any case it is clear that connections among FBGs have a high risk of failure.
In the case you need a fiber with a high number of FBGs on it, the solution is to incise directly onto the virgin fiber. It is clear that this has to be done according with the specifications of the project, namely what kind of measure you want and where you want to make it.

- **Gluing**: it has already been said about the enormous problems about the gluing of the fiber.

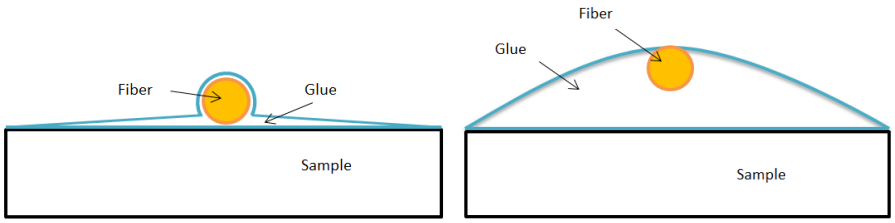

Figure 6.6 - Frontal section of fiber glued, in two cases: the first if you have put a very low layer of glue, and the second if you have put too much glue

At first in order to glue the fiber, you have to pay attention to the quantity of adhesive to apply. If there is low amount of glue, the measures of FBG will be reliable, but it will split soon (Figure 6.6 case a). Instead, if you apply too much glue, the FBG will be protected, but the layer of glue will absorb strain deformations. So the fiber measures will be distorted. To control if the gluing has been made in an optimal way, the sample has been deformed with a deformation of 25mm at the tip. It has been fixed with this configuration for a long time (from 20 to 40 minutes). Once completed the test you control the signal of the FBG: if the loss of the signal is in the order of thousandths of nanometer or at maximum few hundredth of nanometer the gluing is valid.
Also if the gluing has been made in the optimal way, there is always the problem of the unknown position of the fiber which have been mentioned before. You need to be able to press down the fiber to hold it in contact with the sample, without being joint with them.
In order to achieve it, a slim film in PE (Polyethylene) has been placed over the layer of glue. Then a heavy and smooth mass has been laid over all. This ensures to pull the fiber on the sample and the film in PE (or in PVC) does not allow to the mass to remain glued.

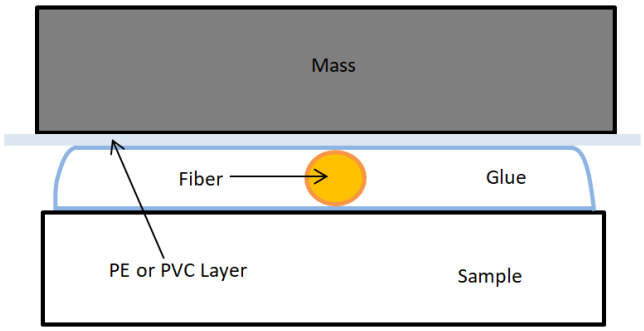

Figure 6.7 - Scheme of the elements and their application to make the new typology of gluing

The tests with this method of gluing are in the subchapter "1F_1B test - Sample with one Fiber and one Bragg Grating, with Alternative Gluing Method" and in Appendix A there are more cases with this sample. The gluing of the FBG has been made in our lab.

Figure 6.8 - Sample with FBG (in line with the piece of white paper), a layer of glue and the film in PE over all

The tests, with the results, confirm the excellent qualities of this process of gluing. Furthermore, this method brings also an unexpected benefit: the resin, to polymerise perfectly, needs pressure on itself, and this method does this.
The last point deals with the ageing of the glue. After 40-50 days from the gluing the resistance starts to give up.

For future works regarding the FBG placed with this configuration, there are a lot of possible studies to carry out. The seal of the glue for a long time, more extreme tests with also breaking tests and fatigues tests, both

for the glue and the FBGs, behaviour of the aggregate with variation of temperature and other set to fix the FBGs.

Appendix A - Database of the tests

These tests have been made on the 08th February 2019

Table 17 - Microstrains recorded by the FBGs of the 2F_2B sample, made on the 08th February 2019

Displacement imposed to the tip	Strain recorded by the FBG [$\mu\epsilon$]			
	F1 - B1	F1 - B2	F2 - B1	F2 - B2
2 mm	13,46	21,043	9,177	19,759
4 mm	23,696	39,752	18,46	39,42
6 mm	33,141	57,475	27,171	57,954
8 mm	42,933	76,763	36,148	77,553
10 mm	53,285	96,588	45,905	96,021
12 mm	62,643	115,267	57,045	116,012
14 mm	73,094	135,261	66,798	135,522
16 mm	82,545	153,656	75,512	154,555
18 mm	92,146	175,259	83,986	173,615
20 mm	105,134	194,516	93,073	193,542

Table 18 - Percentage error of the Bragg #1 and Bragg #2 respect the values from Nastran - Patran of the 2F_2B sample, made on the 08th February 2019

Error of the Bragg gratings respect values made by Nastran - Patran #1 [%]		Error of the Bragg gratings respect values made by Nastran - Patran #2 [%]	
Fiber 1	Fiber 2	Fiber 1	Fiber 2
53,83	4,88	9,31	2,64
35,41	5,49	3,25	2,39
26,25	3,51	-0,91	-0,08
22,14	2,84	-0,82	0,20
22,07	5,17	0,09	-0,50
18,75	8,14	-0,50	0,14
18,85	8,61	0,19	0,39
17,67	7,64	-0,48	0,10
16,64	6,31	0,72	-0,22
19,67	5,95	0,79	0,28

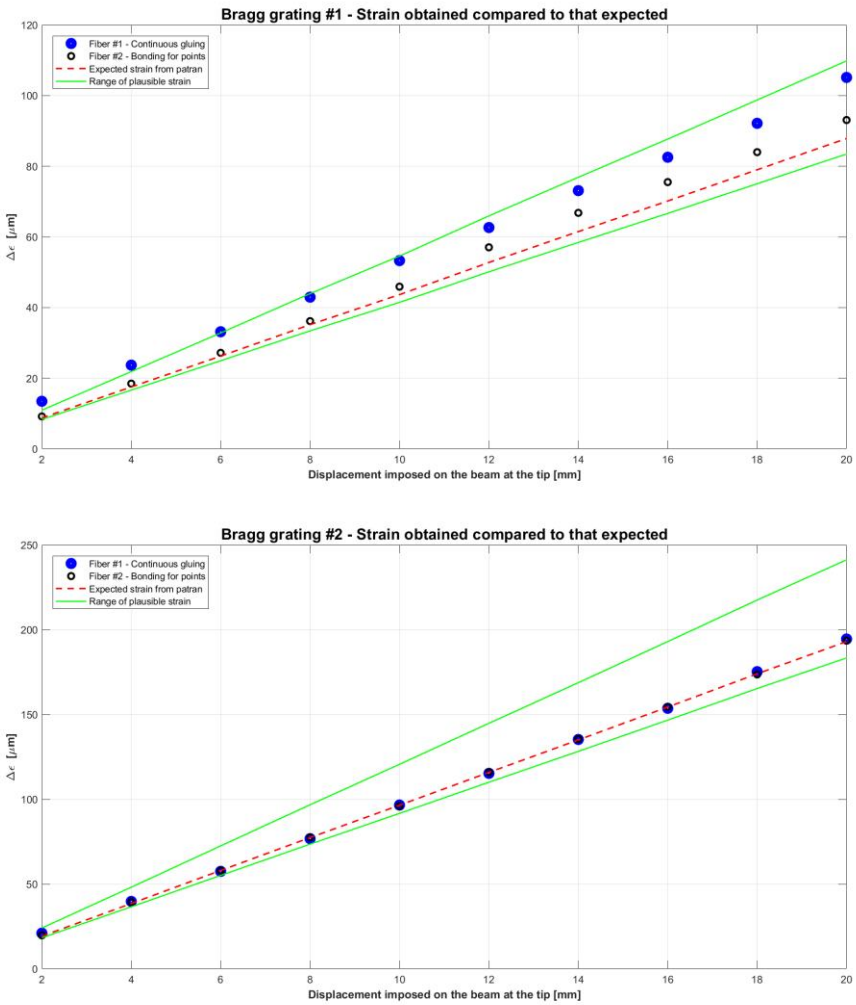

Figure 0.1 - Progress of microstrain, in the Bragg Gratings #1 and in the Bragg Gratings #2, of the two fibers of the 2F_2B sample, made on the 08th February 2019. The red line is the expected value of microstrain in output from Nastran - Patran. Instead, the zone between the green lines, is the range of values plausible, it depends on the thickness of the glue used

The following results have been obtained, instead, on the 12th February 2019

Table 19 - Microstrains recorded by the FBGs of the 2F_2B sample, made on the 12th February 2019

Displacement imposed to the tip	Strain recorded by the FBG [$\mu\epsilon$]			
	F1 - B1	F1 - B2	F2 - B1	F2 - B2
2 mm	8,946	18,082	8,203	17,532
4 mm	20,287	36,973	15,675	36,929
6 mm	29,716	54,556	24,020	54,651
8 mm	38,599	73,388	32,147	73,937
10 mm	47,998	90,949	40,757	91,622
12 mm	57,025	110,997	49,247	110,710
14 mm	66,548	129,300	57,858	129,431
16 mm	75,636	148,423	69,280	149,050
18 mm	85,703	167,650	77,893	167,498
20 mm	95,095	188,567	86,343	186,744

Table 20 - Percentage error of the Bragg #1 and Bragg #2 of the 2F_2B sample, made on the 12th February 2019, respect the values from Nastran - Patran

Error of the Bragg gratings respect values made by Nastran - Patran #1 [%]		Error of the Bragg gratings respect values made by Nastran - Patran #2 [%]	
Fiber 1	Fiber 2	Fiber 1	Fiber 2
2,24	-6,25	-6,07	-8,92
15,93	-10,43	-3,97	-4,08
13,20	-8,50	-5,94	-5,77
9,81	-8,54	-5,18	-4,47
9,96	-6,63	-5,75	-5,05
8,10	-6,64	-4,19	-4,44
8,21	-5,92	-4,22	-4,13
7,82	-1,24	-3,87	-3,47
8,48	-1,40	-3,65	-3,74
8,25	-1,72	-2,30	-3,24

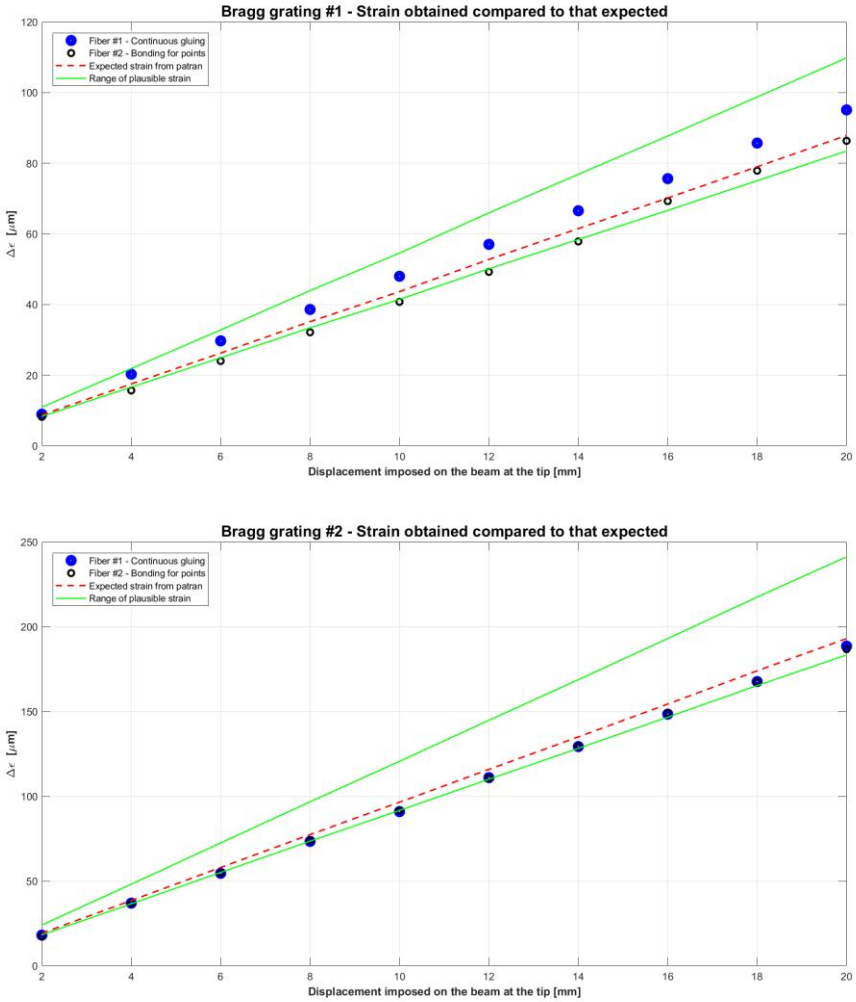

Figure 0.2 - Progress of microstrain, in the Bragg Gratings #1 and in the Bragg Gratings #2, of the two fibers of the 2F_2B sample, made on the 12th February 2019. The red line is the expected value of microstrain in output from Nastran - Patran. Instead, the zone between the green lines, is the range of values plausible, it depends on the thickness of the glue used

Lastly this test has been made on the 15th February 2019

Table 21 - Microstrains recorded by the FBG of the 2F_2B sample, made on the 15th February 2019

Displacement imposed to the tip	Strain recorded by the FBG [$\mu\epsilon$]			
	F1 - B1	F1 - B2	F2 - B1	F2 - B2
2 mm	6,807	15,519	6,270	17,013
4 mm	15,982	33,671	14,399	35,560
6 mm	24,368	51,374	22,107	53,522
8 mm	34,308	68,854	31,200	71,305
10 mm	42,907	88,697	39,177	89,590
12 mm	52,601	106,407	48,886	108,586
14 mm	62,304	126,602	59,528	128,613
16 mm	70,763	144,474	67,180	146,586
18 mm	79,531	165,433	75,099	165,670
20 mm	91,930	183,891	83,802	184,828

Table 22 - Percentage error of the Bragg #1 and Bragg #2 of the 2F_2B sample, made on the 15th February 2019, respect the values from Nastran - Patran

Error of the Bragg gratings respect values made by Nastran - Patran #1 [%]		Error of the Bragg gratings respect values made by Nastran - Patran #2 [%]	
Fiber 1	Fiber 2	Fiber 1	Fiber 2
-22,21	-28,34	-19,38	-11,62
-8,67	-17,72	-12,54	-7,64
-7,17	-15,78	-11,42	-7,72
-2,40	-11,24	-11,04	-7,87
-1,70	-10,25	-8,09	-7,16
-0,28	-7,33	-8,15	-6,27
1,31	-3,21	-6,22	-4,73
0,87	-4,23	-6,43	-5,06
0,67	-4,94	-4,92	-4,79
4,64	-4,61	-4,72	-4,23

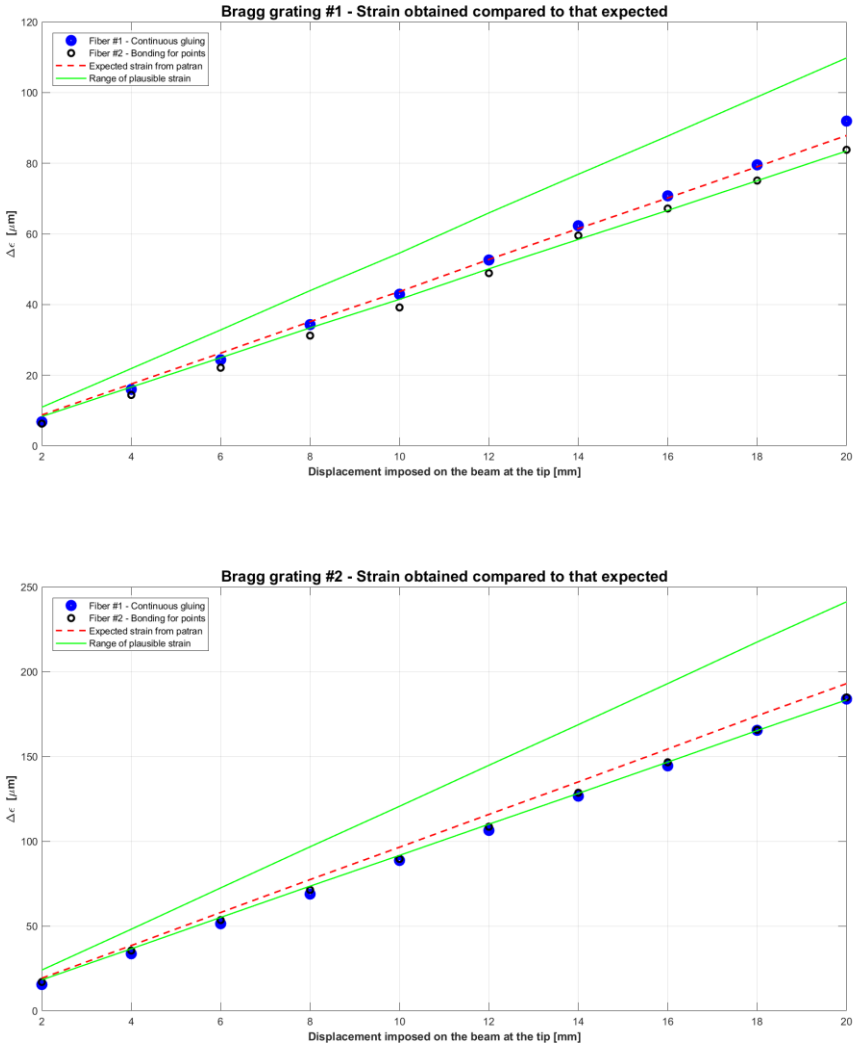

Figure 0.3 - Progress of microstrain, in the Bragg Gratings #1 and in the Bragg Gratings #2, of the two fibers of the 2F_2B sample, made on the 15th February 2019. The red line is the expected value of microstrain in output from Nastran - Patran. Instead, the zone between the green lines, is the range of values plausible, it depends on the thickness of the glue used

The following tests are with the sample 1F_1B.
In particular the test made on the 22nd February 2019 gives in output:

Table 23 - Microstrains recorded by the FBG of the 1F_1B sample, made on the 22nd February 2019

Displacement imposed to the tip	Strain recorded by the FBG [$\mu\epsilon$]	Error of the Bragg gratings respect values made by Nastran - Patran [%]
	F1 - B1	
2 mm	15,816	-6,96
4 mm	31,458	-7,48
6 mm	48,285	-4,39
8 mm	64,652	-4,22
10 mm	81,078	-4,05
12 mm	96,302	-5,12
14 mm	112,94	-4,45
16 mm	128,461	-4,84
18 mm	144,949	-4,64
20 mm	161,311	-4,55

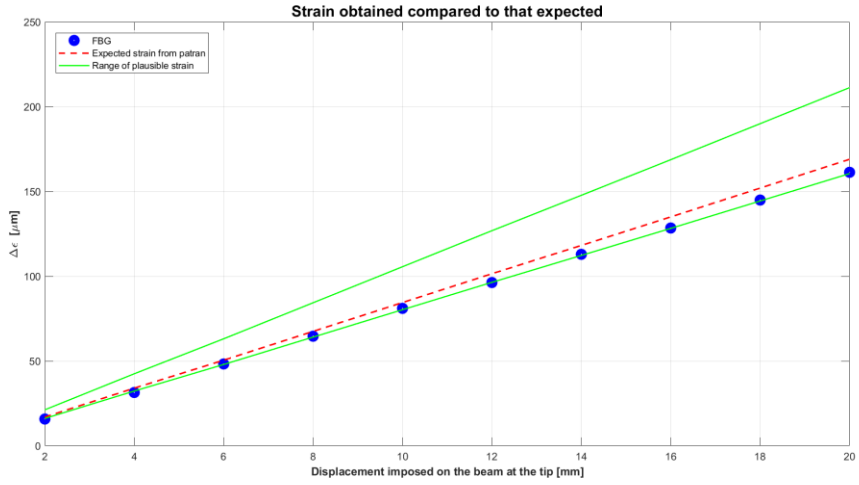

Figure 0.4 - Progress of microstrain, in the Bragg Gratings of the 1F_1B sample, made on the 22nd February 2019. The red line is the expected value of microstrain in output from Nastran - Patran. Instead, the zone between the green lines, is the range of values plausible, it depends on the thickness of the glue used

These tests instead are made on the 27th February 2019:

Table 24 - Microstrains recorded by the FBG of the 1F_1B sample, made on the 27th February 2019

Displacement imposed to the tip	Strain recorded by the FBG [$\mu\epsilon$]	Error of the Bragg gratings respect values made by Nastran - Patran [%]
	F1 - B1	
2 mm	16,919	-0,48
4 mm	36,145	6,31
6 mm	52,509	3,98
8 mm	68,945	2,14
10 mm	84,98	0,57
12 mm	102,053	0,54
14 mm	118,325	0,11
16 mm	134,276	-0,54
18 mm	149,854	-1,41
20 mm	166,174	-1,67

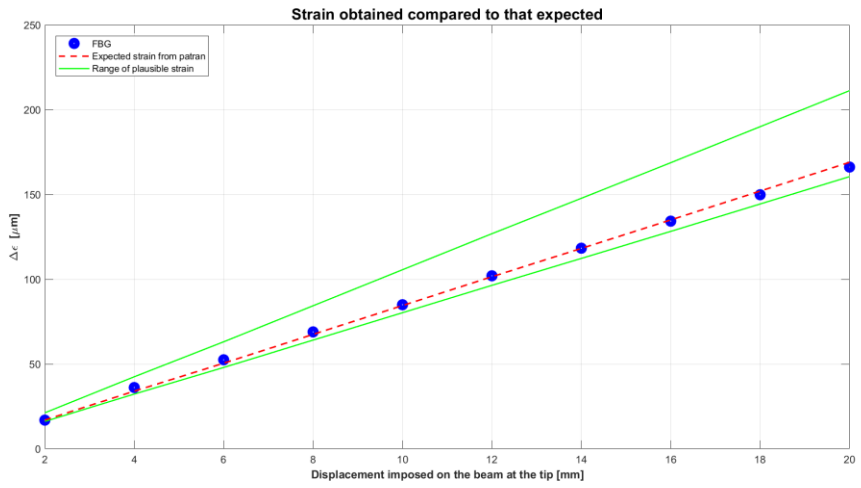

Figure 0.5 - Progress of microstrain, in the Bragg Gratings of the 1F_1B sample, made on the 27nd February 2019. The red line is the expected value of microstrain in output from Nastran - Patran. Instead, the zone between the green lines, is the range of values plausible, it depends on the thickness of the glue used

The following test is made on the 04th March 2018

Table 25 - Microstrain recorded by the FBG of the 1F_1B sample, made on the 4th March 2019

Displacement imposed to the tip	Strain recorded by the FBG [$\mu\epsilon$]	Error of the Bragg gratings respect values made by Nastran - Patran [%]
	F1 - B1	
2 mm	15,931	-6,29
4 mm	30,983	-8,87
6 mm	46,617	-7,69
8 mm	62,353	-7,63
10 mm	78,292	-7,35
12 mm	94,628	-6,77
14 mm	110,755	-6,3
16 mm	128,56	-4,77
18 mm	145,545	-4,25
20 mm	162,54	-3,82

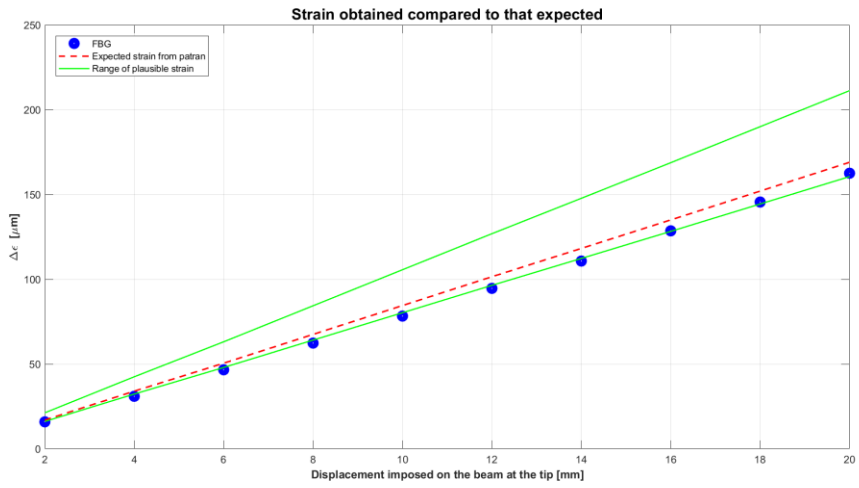

Figure 0.6 - Progress of microstrain, in the Bragg Gratings of the 1F_1B sample, made on the 4th March 2019. The red line is the expected value of microstrain in output from Nastran - Patran. Instead, the zone between the green lines, is the range of values plausible, it depends on the thickness of the glue used

Appendix B - Structural analysis

If a stress is applied on a generic casing, it will cause a deformation. This deformation could be in the elastic or plastic field. In the elastic field the deformation is reversible; instead in the plastic one the deformation is permanent.
Our tests are always unfolded in the elastic field.
However, for some analytic calculations, it is possible to use the Euler-Bernoulli Beam Theory. At first all our samples are assumed like a beam, namely an elongated solid where the dimensions of transversal section are unimportant respect to the length. Secondly, in the Euler-Bernoulli Theory, that is a simplification of the problem of De Saint Venant, the sections remain plane during the deformation and orthogonal to the longitudinal axis. Furthermore, the sections must not have big variations along the longitudinal axis.
Going further, if our solid is submitted to a stress it will have a deformation. The mechanical strain, object of this thesis, is defined like ϵ:

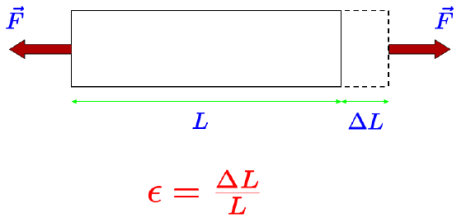

Figure 0.1 - Mechanical strain

When you have a bending strains of a beam, you will have traction on a surface and compression on the other (Figure 6.1 - Section of the group sample and fiber glued together, page 63). It is possible to find the normal stress with the equation of Navier:

$$\sigma_z = \frac{M_x^f}{I_{xx}} y \tag{18}$$

It is valid in the assumption of De Saint Venant theory.
Being subjected in elastic field we can find:

$$\sigma = E\epsilon \tag{19}$$

References

[1] Guaraglia D. O., Pousa J. L., *Introduction to Modern Instrumentation - For Hydraulics and Environmental Sciences,* De Gruyter, 2014, 8 Groung-Based Remote Sensing System, pp. 273 - 324.
[2] Chandra P., *Nanobiosensors for Personalized and Onsite Biomedical Diagnosis,* Institution of Engineering and Technology, 2016, Fibre optical technology for monitoring and diagnostic applications.
[3] Kasap S., *Optoelectronics and Photonics: Principles and Practise*, Pearson Education Limited, 2013
[4] Candiano G., *Fiber Bragg Grating Sensors for Mechanical and Thermal Prognostic and Diagnostics for Aerospace Applications*, 2018
[5] Donà R., Zoccoli A., *Proposta dell'esperimento FIBRAGG (Fiber BRAGg Grating)*, 2009
[6] *SmartScan Product Manual*
[7] Tosi D., Perrone G., *Fiber-Optic Sensors for Biomedical Applications*, Artech House, 2018
[8] Broker G., *Introduction to mechatronics*, SciTech Publishing, 2012
[9] Agrawal P., *Application of nonlinear fiber optics* 2^{nd} *Edition*, Elsevier, 2008